Electronic Supplementary Material (ESI) for Materials Advances.

Supporting Information

Alkoxy Phosphonic Acid-Functionalized Conjugated Microporous Polymers for Efficient and Multi-environmental Proton Conduction

Kaijie Yang,[a] Yuxiang Wang,[a] Zhiyi Ling,[a] Xiaogang Pan,[b] Gen Zhang*,[a] and Jian Su*,[a, c]

[a]Key Laboratory for Soft Chemistry and Functional Materials of Ministry of Education, School of Chemistry and Chemical Engineering, Nanjing University of Science and Technology, Nanjing, Jiangsu 210094, China

[b]School of Electrical Engineering, Southeast University, Nanjing, Jiangsu 210096, China

[c]State Key Laboratory of Coordination Chemistry, Nanjing University, Nanjing, Jiangsu 210023, China

*Corresponding author. E-mail: zhanggen@njust.edu.cn (G. Z.); sujian@njust.edu.cn (J. S.)

Table of contents

1. Materials and methods

All the chemicals are commercially available, and used without further purification. All solvents were dried and distilled according to conventional methods.

Powder X-ray diffraction (PXRD): PXRD patterns were collected on a Bruker D8 ADVANCE diffractometer using Cu Kα radiation (λ = 1.5418 Å). High resolution synchrotron powder diffraction data were collected using beamline 17-BM at the Advanced Photon Source (APS), Argonne National Laboratory using an average wavelength of 0.45187 Å. Discrete detectors covering an angular range from −6 to 16º (2theta) are scanned over a 34º (2theta) range, with data points collected every 0.001º 2 theta and scan speed of 0.01º/s. Data were taken at 400, 700, and 1000 mm.

Fourier transform infrared (FT-IR): FT-IR spectra was measured on a Thermo Fisher Scientific Optics NICOLETIS10 FT-IR spectrometer with Universal ATR accessory between the ranges of 4000 to 500 cm^{-1}.

Solution nuclear magnetic resonance (sNMR): Liquid state ^{1}H nuclear magnetic resonance spectra was collected on a Bruker Avance III instrument with AS500 magnet equipped with a cryoprobe (500 MHz). Liquid state ^{13}C nuclear magnetic resonance spectra were measured on a Bruker Advance III instrument with AS500 magnet equipped with a cryoprobe (125 MHz). Liquid state ^{31}P nuclear magnetic resonance spectra were measured on a Bruker Advance III instrument with AS500 magnet equipped with a cryoprobe (202.41 MHz).

Scanning electron microscope (SEM): SEM images were collected using a JSM-IT500HR system, JEOL.

Transmission electron microscope (TEM): TEM images were collected using a JEM-2100, JEOL.

Solid-state nuclear magnetic resonance (ssNMR): Solid state ^{13}C cross-polarization magic-angle-spinning (CP/MAS) NMR spectra were recorded on a JEOL JNM-ECA 400 MHz, 4.0 mm rotor, MAS of 10 kHz, recycle delay of 1 sec.

High resolution mass spectrometry (HRMS): HRMS mass spectra were

collected on a Baird Acquity UPLC/XEVO G2-XS QTOF using $CHCl_3$ as a solvent.

Thermogravimetric analysis (TGA): TGA was performed using a NETZSCH STA 449F5 under flowing N_2 (60 mL min^{-1}) with 10 K min^{-1} ramp rate. Samples were heated in a Platinum pan from 50 °C to 900 °C (10 °C min^{-1}).

Gas adsorption: N_2 adsorption and desorption measurements were performed at 77 K using BEL (MicrotracBEL Corp, Japan), before gas adsorption measurements, all the solids have been dried at 80 °C under vacuum in a drying oven for 24 h to remove residual solvent, then all the samples have been degassed under vacuum at 100 °C with BELPREP VAC III for 12 h to afford the sample for sorption analysis. The pore size distributions of samples in this work were estimated by Nonlocal Density Functional Theory (NLDFT) based on the model of N_2/77 K on graphitic carbon with slit pores and the method of Tikhonov regularization.

Water vapor adsorption and desorption measurements were performed at 298 K using BEL (MicrotracBEL Corp, Japan).

The water contact angles (WAC): the water contact angles were measured on goniometer (JC2000C, Japan) equipped with video capture.

X-ray photoelectron spectroscopy (XPS): X-ray photoelectron spectroscopy (XPS) spectra were measured with the kratos axis supra^{TM} of Shimadzu.

2. Synthesis

2.1.Synthesis of monomer S3.

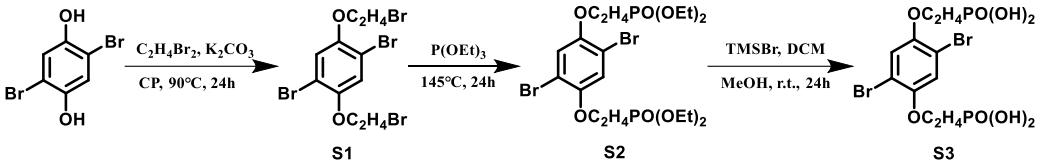

1,4-dibromo-2,5-bis(2-bromoethoxy)benzene (S1). S1 was synthesized according to the reported literature with a modified procedure [1]. 2,5-dibromohydroquinone (2.679 g, 10.00 mmol), 1,2-dibromoethane (2.59 mL, 30.00 mmol), and potassium carbonate (6.911 g, 50.00 mmol) were dissolved in anhydrous acetone (50.00 mL). The resulting solution was refluxed overnight at 90 °C under argon atmosphere. The resulting mixture was concentrated under vacuum and then redissolved in dichloromethane and washed with water. After water was dried over $MgSO_4$ and dichloromethane was removed under vacuum, the crude product was purified with silica-gel column chromatography (petroleum ether/dichloromethane = 2:1, v/v) to give 3.919 g of **S1** in 81.3% yield as a white powder. **^{1}H NMR** ($CDCl_3$, 500 MHz) δ (ppm): 7.14 (s, 2H), 4.29 (t, 4H), 3.66 (t, 4H); **^{13}C NMR** ($CDCl_3$, 125 MHz) δ (ppm): 150.07, 119.80, 111.88, 70.34, 28.38.

tetraethyl (((2,5-dibromo-1,4-phenylene)bis(oxy))bis(ethane-2,1-diyl))bis(phosphonate) (S2). S1 (1.500 g, 3.11 mmol), triethyl phosphite (4.27 mL, 24.90 mmol) were added into a 50.00 mL round-bottom flask. The resulting solution was refluxed for 24h at 145 °C. The resulting mixture was redissolved in dichloromethane and washed with water. After water was dried over $MgSO_4$ and dichloromethane was removed under vacuum, the crude product was purified with silica-gel column chromatography (ethyl acetate) to give 1.334g of **S2** in 71.9% yield as a white powder. **^{1}H NMR** ($CDCl_3$, 500 MHz) δ (ppm): 4.13 (t, 4H), 2.34 (m, 4H), 1.35 (t, 12H); **^{13}C NMR** ($CDCl_3$, 125 MHz) δ (ppm): 149.89, 119.07, 111.40, 64.63, 62.03, 29.73, 16.52.

(((2,5-dibromo-1,4-phenylene)bis(oxy))bis(ethane-2,1-diyl))bis(phosphonic

acid) (S3). S2 (0.994 g, 1.67 mmol) and bromotrimethylsilane (2.64 mL, 20.01 mmol) were added into anhydrous dichloromethane (25.00 mL). The resulting solution was stirred for 12h at room temperature under argon atmosphere. Methanol (50.00 mL) was added into the resulting solution. The mixture was stirred for 12 h at room temperature. The resulting mixture was concentrated under vacuum and dried at 80 °C under vacuum for 12 h to give 0.719 g of **S3** in 89.1% yield as a white powder. **^{1}H NMR** (DMSO, 500 MHz) δ (ppm): 8.93(s, 4H), 7.37 (s, 2H), 4.17 (t, 4H), 2.07 (t, 4H); **^{13}C NMR** (DMSO, 125 MHz) δ (ppm): 149.50, 119.20, 111.14, 65.62, 29.06; **^{31}P NMR** (DMSO, 202.41 MHz) δ (ppm): 38.07; **ESI-HRMS**: calcd. for [$C_{10}H_{14}Br_2O_8P_2$ – H] 482.85102; found 482.84451.

2.2.Synthesis of monomer S6.

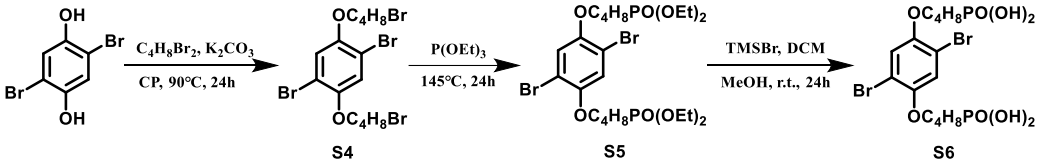

1,4-dibromo-2,5-bis(4-bromobutoxy)benzene (S4). S4 was synthesized according to the reported literature with a modified procedure. 2,5-dibromohydroquinone (2.679 g, 10.00 mmol), 1,4-dibromobutane (3.58 mL, 30.00 mmol), and potassium carbonate (6.911 g, 50.00 mmol) were dissolved in anhydrous acetone (50.00 mL). The resulting solution was refluxed overnight at 90 °C under argon atmosphere. The resulting mixture was concentrated under vacuum and then redissolved in dichloromethane and washed with water. After water was dried over $MgSO_4$ and dichloromethane was removed under vacuum, the crude product was purified with silica-gel column chromatography (petroleum ether/dichloromethane = 2:1, v/v) to give 4.330 g of **S4** in 80.5% yield as a white powder. **^{1}H NMR** ($CDCl_3$, 500 MHz) δ (ppm): 7.08 (s, 2H), 3.99 (t, 4H), 3.52 (t, 4H), 2.11 (m, 4H), 1.97 (m, 4H); **^{13}C NMR** ($CDCl_3$, 125 MHz) δ (ppm): 150.16, 118.60, 111.35, 69.36, 33.71, 29.60, 27.90.

tetraethyl (((2,5-dibromo-1,4-phenylene)bis(oxy))bis(butane-4,1-diyl))bis(phosphonate) (S5). S4 (1.50 g, 2.79 mmol), triethyl phosphite (3.80 mL, 22.3 mmol) were added into a 50.00 mL round-bottom flask. The resulting solution was

refluxed for 24h at 145 °C. The resulting mixture was redissolved in dichloromethane and washed with water. After water was dried over $MgSO_4$ and dichloromethane was removed under vacuum, the crude product was purified with silica-gel column chromatography (ethyl acetate) to give 1.332g of **S5** in 73.2% yield as a white powder. **^{1}H NMR** ($CDCl_3$, 500 MHz) δ (ppm): 7.07 (s, 2H), 4.09 (m, 8H), 3.97 (t, 4H), 1.91 (m, 4H), 1.84 (m, 8H), 1.32 (t, 12H); **^{13}C NMR** ($CDCl_3$, 125 MHz) δ (ppm): 150.18, 118.66, 111.34, 69.68, 61.66, 26.10, 24.98, 19.52, 16.65.

(((2,5-dibromo-1,4-phenylene)bis(oxy))bis(butane-4,1-diyl))bis(phosphonic acid) (S6). S5 (1.240 g, 1.90 mmol) and bromotrimethylsilane (3.01 mL, 22.8 mmol) were added into anhydrous dichloromethane (30.00 mL). The resulting solution was stirred for 12h at room temperature under argon atmosphere. Methanol (50.00 mL) was added into the resulting solution. The mixture was stirred for 12 h at room temperature. The resulting mixture was concentrated under vacuum and dried at 80 °C under vacuum for 12 h to give 0.927 g of **S6** in 86.7% yield as a white powder. **^{1}H NMR** (DMSO, 500 MHz) δ (ppm): 7.35 (s, 2H), 4.00 (t, 4H), 3.39 (s, 4H), 1.77 (m, 4H), 1.63 (t, 4H), 1.55 (m, 4H); **^{13}C NMR** (DMSO, 125 MHz) δ (ppm): 149.50, 118.28, 110.56, 69.35, 27.86, 26.77, 19.61; **^{31}P NMR** (DMSO, 202.41 MHz) δ (ppm): 43.80; **ESI-HRMS**: calcd. for [$C_{14}H_{22}Br_2O_8P_2$ – H] 538.91362; found 538.90726.

2.3.Synthesis of monomer S9.

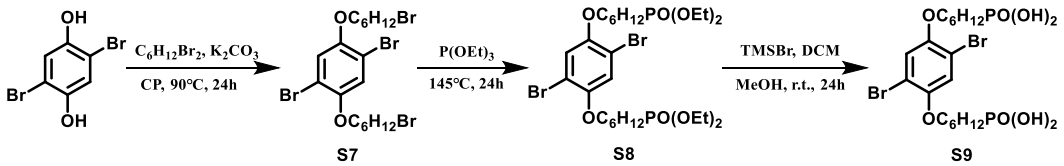

1,4-dibromo-2,5-bis((6-bromohexyl)oxy)benzene (S7). S7 was synthesized according to the reported literature with a modified procedure. 2,5-dibromohydroquinone (2.679 g, 10.00 mmol), 1,6-dibromohexane (4.15 mL, 27.00 mmol), and potassium carbonate (6.911 g, 50.00 mmol) were dissolved in anhydrous acetone (50.00 mL). The resulting solution was refluxed overnight at 90 °C under argon atmosphere. The resulting mixture was concentrated under vacuum and then redissolved in dichloromethane and washed with water. After water was dried over

$MgSO_4$ and dichloromethane was removed under vacuum, the crude product was purified with silica-gel column chromatography (petroleum ether/dichloromethane = 2:1, v/v) to give 4.728 g of **S7** in 79.6% yield as a white powder. **^{1}H NMR** (500 MHz, $CDCl_3$, ppm) δ: 7.07 (s, 2H), 4.08 (t, 4H), 3.52 (t, 4H), 1.80 (m, 4H), 1.73 (m, 4H), 1.48 (m, 4H), 1.31 (m, 4H); **^{13}C NMR** ($CDCl_3$, 125 MHz) δ (ppm): 150.21, 118.61, 111.30, 70.24, 33.62, 32.21, 29.06, 25.73, 25.24.

tetraethyl (((2,5-dibromo-1,4-phenylene)bis(oxy))bis(hexane-6,1-diyl))bis(phosphonate) (S8). S7 (1.50 g, 2.53 mmol), triethyl phosphite (3.46 mL, 20.2 mmol) were added into a 50.00 mL round-bottom flask. The resulting solution was refluxed for 24h at 145 °C. The resulting mixture was redissolved in dichloromethane and washed with water. After water was dried over $MgSO_4$ and dichloromethane was removed under vacuum, the crude product was purified with silica-gel column chromatography (ethyl acetate) to give 1.332g of **S8** in 73.2% yield as a white powder. **^{1}H NMR** (500 MHz, $CDCl_3$, ppm) δ: 7.07 (s, 2H), 4.10 (m, 8H), 3.94 (t, 4H), 1.81 (m, 4H), 1.73 (t, 4H), 1.52 (m, 4H), 1.46 (m, 4H), 1.32 (t, 12H), 1.26 (m, 4H); **^{13}C NMR** ($CDCl_3$, 125 MHz) δ (ppm): 150.26, 118.68, 111.35, 70.28, 61.64, 29.06, 26.37, 25.72, 25.26, 22.59, 16.71.

(((2,5-dibromo-1,4-phenylene)bis(oxy))bis(hexane-6,1-diyl))bis(phosphonic acid) (S9). S8 (0.200 g, 0.28 mmol) and bromotrimethylsilane (0.45 mL, 3.38 mmol) were added into anhydrous dichloromethane (10.00 mL). The resulting solution was stirred for 12h at room temperature under argon atmosphere. Methanol (50.00 mL) was added into the resulting solution. The mixture was stirred for 12 h at room temperature. The resulting mixture was concentrated under vacuum and dried at 80 °C under vacuum for 12 h to give 0.144 g of **S9** in 85.3% yield as a white powder. **^{1}H NMR** (DMSO, 500 MHz) δ (ppm): 10.02 (s, 4H),7.33 (s, 2H), 3.99 (t, 4H), 1.68 (m, 4H), 1.50 (t, 4H), 1.48 (m, 4H), 1.45 (m, 4H), 1.40 (m, 4H); **^{13}C NMR** (DMSO, 125 MHz) δ (ppm): 149.49, 118.26, 110.58, 69.58, 29.80, 28.46, 27.05, 25.16, 22.82; **^{31}P NMR** (DMSO, 202.41 MHz) δ (ppm): 44.31; **ESI-HRMS**: calcd. For [$C_{18}H_{30}Br_2O_8P_2$ – H] 594.97622; found 594.96974.

2.4.Synthesis of Monomer S12.

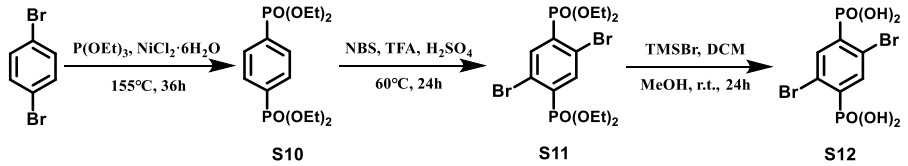

tetraethyl 1,4-phenylenebis(phosphonate) (S10). S10 was synthesized according to the reported literature with a modified procedure [2]. 1,4-dibromobenzene (2.00 g, 8.48 mmol), triethyl phosphite (8.72 mL, 50.88 mmol), $NiCl_2·6H_2O$ (0.400 g, 1.70 mmol) were added into a 50.00 mL round-bottom flask. The resulting solution was refluxed for 48h at 150 °C. The resulting mixture was redissolved in dichloromethane and washed with water. After water was dried over $MgSO_4$ and dichloromethane was removed under vacuum, the crude product was purified with silica-gel column chromatography (ethyl acetate) to give 1.675g of **S10** in 56.4% yield as a white powder. **^{1}H NMR** ($CDCl_3$, 500 MHz) δ (ppm): 7.88 (s, 4H), 4.12 (m, 8H), 1.32 (t, 12H); **^{13}C NMR** ($CDCl_3$, 125 MHz) δ (ppm): 131.89, 62.77, 16.63.

tetraethyl (2,5-dibromo-1,4-phenylene)bis(phosphonate) (S11). A 50 mL round-bottom flask was charged with **S10** (0.981 g, 2.80 mmol), trifluoroacetic acid (20.0 mL), and concentrated H_2SO_4 (6.0 mL). The reaction mixture was heated to 60 °C, and N-bromosuccinimide (1.50 g, 8.43 mmol) was added in portions (250 mg/h) over 6 hours. The stirring was continued for 48 hours at 60 °C, and the reaction mixture was poured into iced water. Yellow precipitate was collected by filtration and were recrystallized twice in ethanol to give 1.154 g of **S11** in 81.1% yield as a white powder. **^{1}H NMR** ($CDCl_3$, 500 MHz) δ (ppm): 7.93 (s, 2H), 4.20 (m, 8H), 1.35 (t, 12H); **^{13}C NMR** ($CDCl_3$, 125 MHz) δ (ppm):133.47, 131.87, 119.97, 62.75, 16.61.

(2,5-dibromo-1,4-phenylene)bis(phosphonic acid) (S12). S11 (1.00 g, 2.85 mmol) and bromotrimethylsilane (3.01 mL, 22.84 mmol) were added into anhydrous dichloromethane (25.00 mL). The resulting solution was stirred for 12h at room temperature under argon atmosphere. Methanol (50.00 mL) was added into the resulting solution. The mixture was stirred for 12 h at room temperature. The resulting mixture was concentrated under vacuum and dried at 80 °C under vacuum for 12 h to give 0.892

g of **S12** in 78.9% yield as a white powder. **^{1}H NMR** (DMSO, 500 MHz) δ (ppm): 7.75 (s, 2H), 7.10 (s, 4H); **^{13}C NMR** (DMSO, 125 MHz) δ (ppm): 138.63, 130.33, 118.43; **^{31}P NMR** (DMSO, 202.41 MHz) δ (ppm): 29.24; **ESI-HRMS**: calcd. For [$C_6H_6Br_2O_6P_2$ – H] 394.79859; found 394.79181.

2.5.Synthesis of Monomer S14.

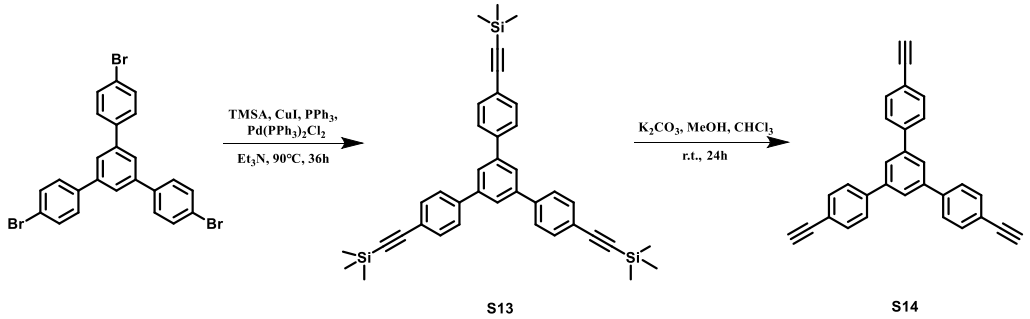

S13 S14

1,3,5-tris-[(4-trimethylsiylethynyl)phenyl]benzene (S13). S13 and **S14** was synthesized according to the reported literature. 1,3,5-tris(4-bromophenyl)benzene (0.300 g, 0.55 mmol), CuI (0.003 g, 0.016 mmol), triphenyl phosphine (0.014 g, 0.055 mmol) and $Pd(PPh_3)_2Cl_2$ (0.019 g, 0.027 mmol) were taken in 100 mL two-neck round bottom flask under nitrogen atmosphere. Then dry and degassed triethylamine (30 mL) was added to this mixture and heated for 30 min at 50°C. Trimethylsilylacetylene (0.34 mL, 2.48 mmol) was added drop wise to the mixture under high nitrogen flow and the reaction mixture was refluxed for 36 h at 90°C. The solvent was removed under vacuum and the crude was purified by column chromatography using 1% ethyl acetate (EA) in hexane mixture to give 0.276 g of **S13** in 84.0% yield as a white powder. **^{1}H NMR** (500 MHz, $CDCl_3$) δ (ppm): 7.74 (s, 3H), 7.63 (d, 6H), 7.57 (d, 6H), 0.28 (s, 27H).

1,3,5-Triethynyltriphenylbenzene (S14). S13 (210 mg, 0.35 mmol) was dissolved in solvent mixture of dichloromethane and methanol (1:2) in 100 mL round bottom flask. Solid potassium carbonate (0.290 g, 2.11 mmol) was added to it and the reaction mixture was stirred for 24 h at room temperature. The solvents were removed under reduced pressure and the crude was purified by column chromatography using hexane as eluent to give 0.122 g of **S14** in 92.0% yield as a light yellow powder. **^{1}H NMR** ($CDCl_3$, 500 MHz) δ (ppm): 7.76 (s, 3H), 7.64 (d, 6H), 7.62 (d, 6H), 3.16 (s, 3H); **^{13}C NMR** ($CDCl_3$, 125 MHz) δ (ppm): 141.89, 141.30, 132.90, 127.41, 125.48, 121.72,

83.60, 78.32.

2.6.Synthesis of CMP-C2-P

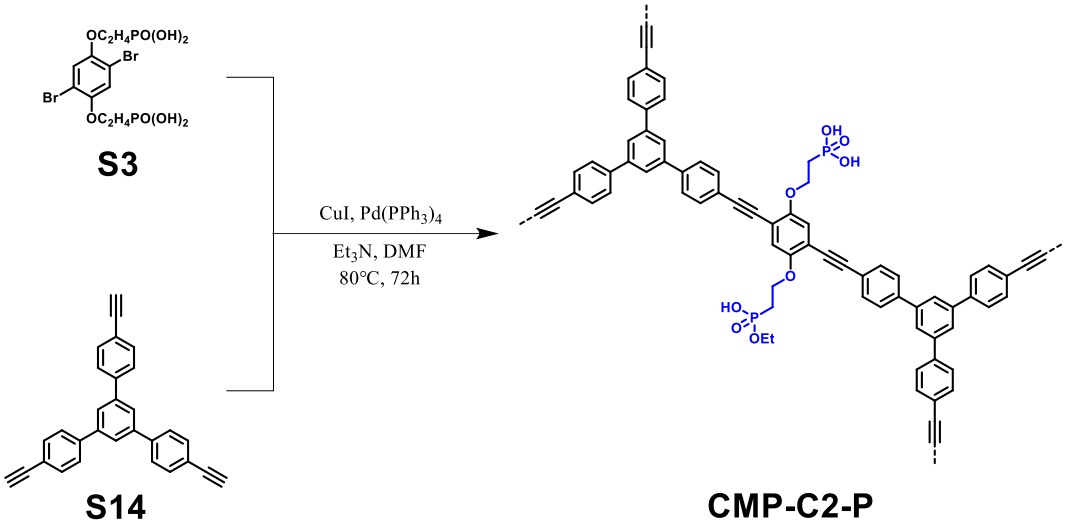

Following the reported literature with a modified procedure [3-6]. **S3** (0.241 g, 0.50 mmol), **S14** (0.126 g, 0.33 mmol), CuI (0.007 g, 0.04 mmol) and $Pd(PPh_3)_4$ (0.022 g, 0.02 mmol) in NEt_3/DMF. The mixture was stirred for 60 h at 80 °C under argon atmosphere and was allowed to cool to room temperature. The crude was washed with dichloromethane (3×10 mL) and acetone (3×10 mL), soaked in dry acetone for 12 h and dried at 80 °C under vacuum for 12 h to give CMP-**C2-P** as a yellow powder (0.329 g, 89.7% yield).

2.7.Synthesis of CMP-C4-P

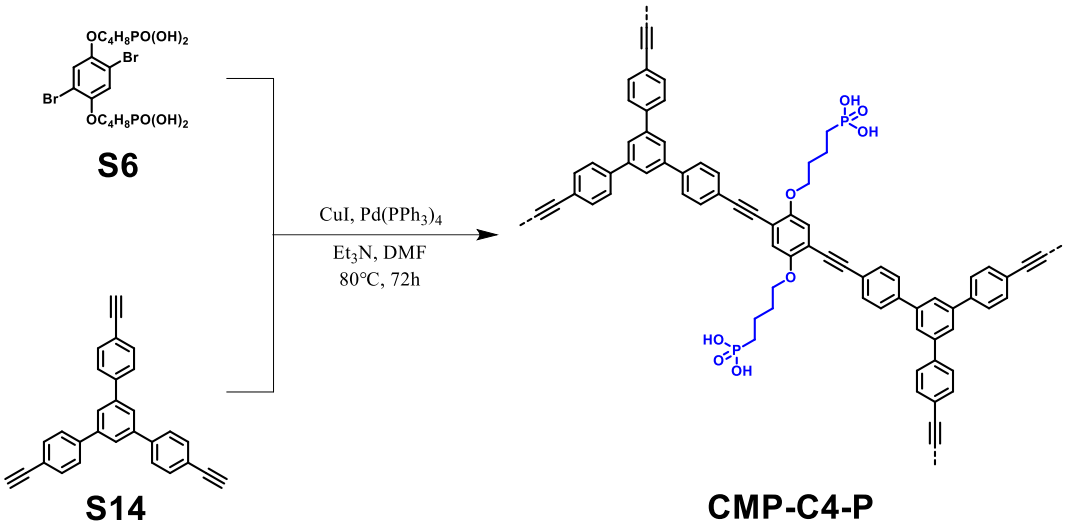

Following the reported literature with a modified procedure. **S6** (0.281 g, 0.50

mmol), **S14** (0.126 g, 0.33 mmol), CuI (0.007 g, 0.04 mmol) and $Pd(PPh_3)_4$ (0.022 g, 0.02 mmol) in NEt_3/DMF. The mixture was stirred for 60 h at 80 °C under argon atmosphere and was allowed to cool to room temperature. The crude was washed with dichloromethane (3×10 mL) and acetone (3×10 mL), soaked in dry acetone for 12 h and dried at 80 °C under vacuum for 12 h to give CMP-**C4-P** as a yellow powder (0.352 g, 86.5% yield).

2.8.Synthesis of CMP-C6-P

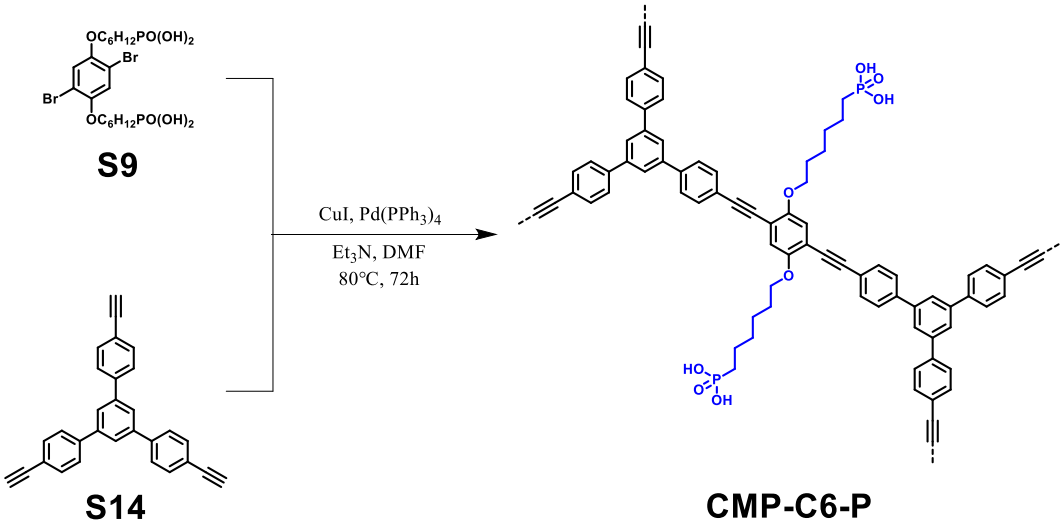

Following the reported literature with a modified procedure. **S9** (0.298 g, 0.50 mmol), **S14** (0.126 g, 0.33 mmol), CuI (0.007 g, 0.04 mmol) and $Pd(PPh_3)_4$ (0.022 g, 0.02 mmol) in NEt_3/DMF. The mixture was stirred for 60 h at 80 °C under argon atmosphere and was allowed to cool to room temperature. The crude was washed with dichloromethane (3×10 mL) and acetone (3×10 mL), soaked in dry acetone for 12 h and dried at 80 °C under vacuum for 12 h to give CMP-**C6-P** as a yellow powder (0.339 g, 80.0% yield).

2.9.Synthesis of CMP-P

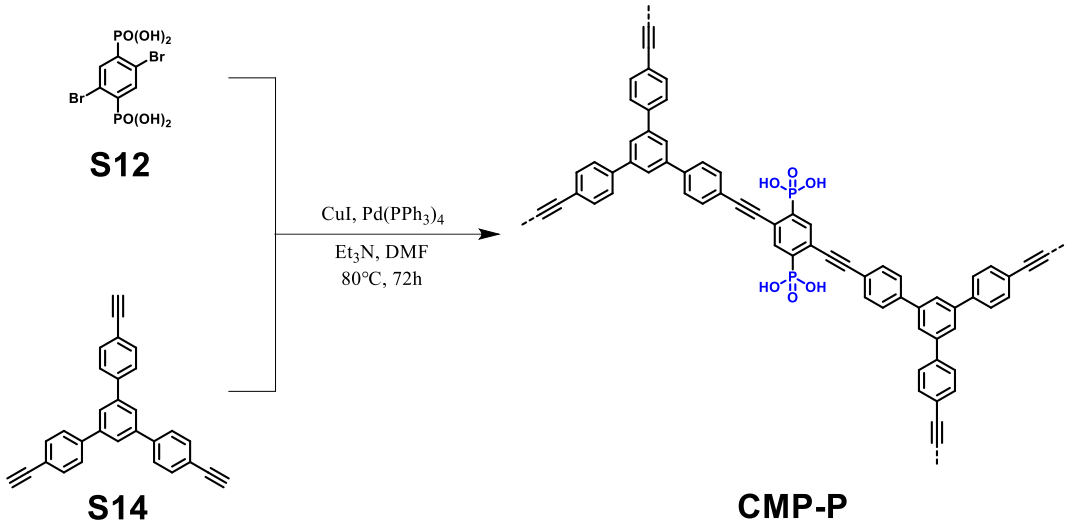

Following the reported literature with a modified procedure. **S12** (0.198 g, 0.50 mmol), **S14** (0.126 g, 0.33 mmol), CuI (0.007 g, 0.04 mmol) and $Pd(PPh_3)_4$ (0.022 g, 0.02 mmol) in NEt_3/DMF. The mixture was stirred for 60 h at 80 °C under argon atmosphere and was allowed to cool to room temperature. The crude was washed with dichloromethane (3×10 mL) and acetone (3×10 mL), soaked in dry acetone for 12 h and dried at 80 °C under vacuum for 12 h to give CMP**-P** as a yellow powder (0.229 g, 70.8% yield).

2.10. Synthesis of CMP-C2S-P

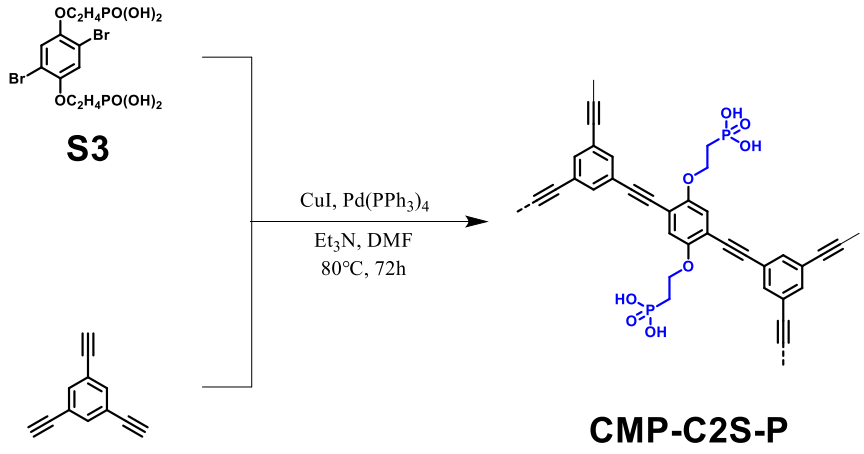

Following the reported literature with a modified procedure. **S3** (0.241 g, 0.50 mmol), 1,3,5-triethynylbenzene (0.050 g, 0.33 mmol), CuI (0.007 g, 0.04 mmol) and $Pd(PPh_3)_4$ (0.022 g, 0.02 mmol) in NEt_3/DMF. The mixture was stirred for 60 h at 80 °C under argon atmosphere and was allowed to cool to room temperature. The crude was

washed with dichloromethane (3×10 mL) and acetone (3×10 mL), soaked in dry acetone for 12 h and dried at 80 °C under vacuum for 12 h to give CMP-**C2S-P** as a yellow powder (0.223 g, 76.6% yield).

2.11. Synthesis of CMP-U

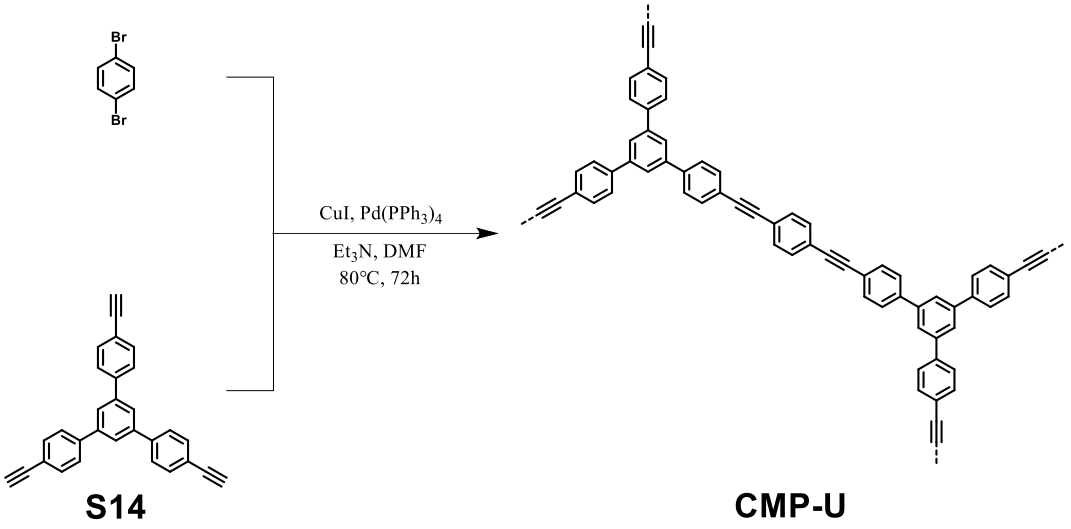

Following the reported literature with a modified procedure. 1,4-dibromobenzene (0.118 g, 0.50 mmol), **S14** (0.126 g, 0.33 mmol), CuI (0.007 g, 0.04 mmol) and $Pd(PPh_3)_4$ (0.022 g, 0.02 mmol) in NEt_3/DMF. The mixture was stirred for 60 h at 80 °C under argon atmosphere and was allowed to cool to room temperature. The crude was washed with dichloromethane (3×10 mL) and acetone (3 ×10 mL), soaked in dry acetone for 12 h and dried at 80 °C under vacuum for 12 h to give CMP-**U** as a yellow powder (212 mg, 87.0% yield).

2.12. H_3PO_4 doping

H_3PO_4 doped CMPs were prepared by manual grinding CMPs and different amount of phosphoric acid. The dried powder samples of CMP-**P** and CMP-**Cx-P** (**x** = **2**, **4**, **6**; **P** stands for phosphonic acid groups) (20 mg) were weighted to an agate mortar, then different amount of neat phosphoric acid was added to the above mortar. After smoothly manual grinding in a mortar with pestle, the solids were collected and dried at 100 °C under vacuum for 12 h. The phosphoric acid doped samples were denoted as CMP-**P-H** and CMP-**Cx-P-H** (**H** represents percentage of phosphoric acid in total mass), respectively. CMP-**C2S-P-H** and CMP-**U-H** were prepared in the same way.

3. Characterization and proton conduction measurements

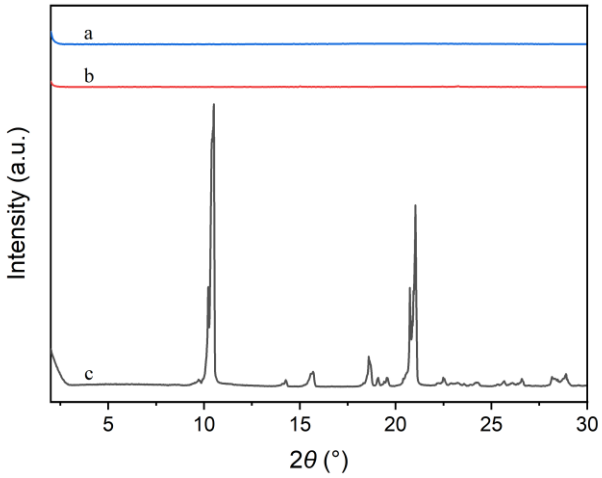

Figure S1. PXRD spectra of (a) CMP-**C2-P**, (b) **S3**, and (c) 1,3,5-triethynyltriphenylbenzene.

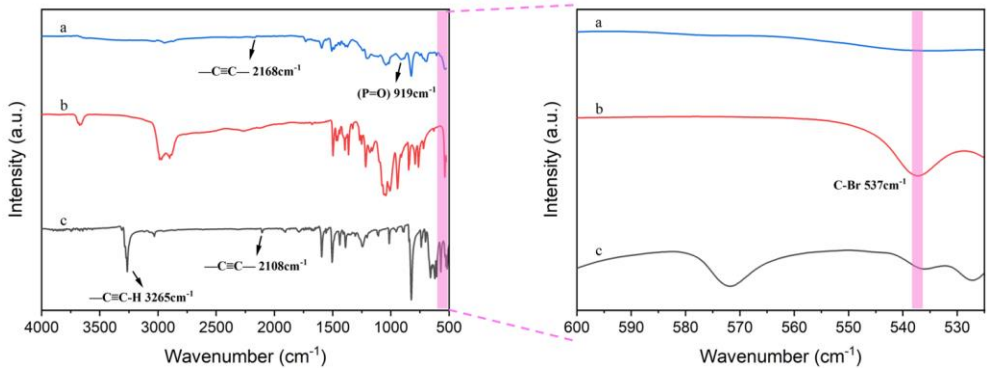

Figure S2. FT-IR spectra of (a) CMP-**C2-P**, (b) **S3**, and (c) 1,3,5-triethynyltriphenylbenzene.

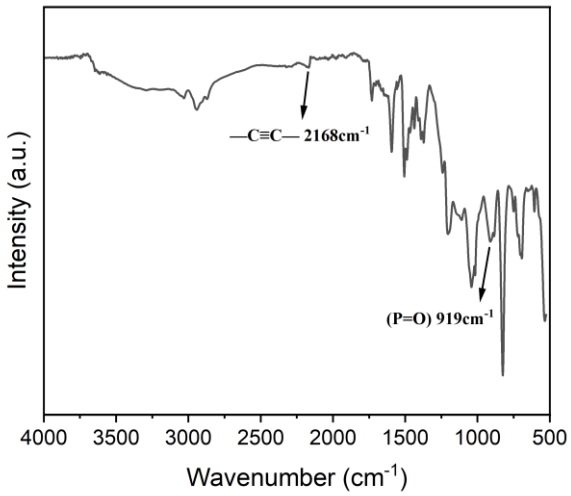

Figure S3. FT-IR spectra of CMP-**C2-P**.

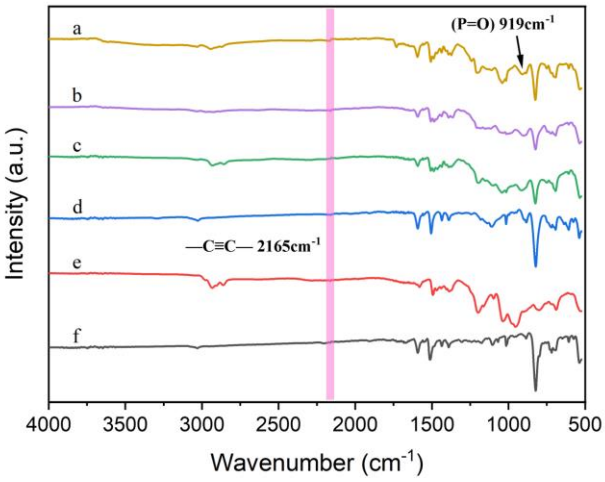

Figure S4. FT-IR spectra of (a) CMP-**C2-P**, (b) CMP-**C4-P**, (c) CMP-**C6-P**, (d) CMP-**P**, (e) CMP-**C2S-P**, and (f) CMP-**U**.

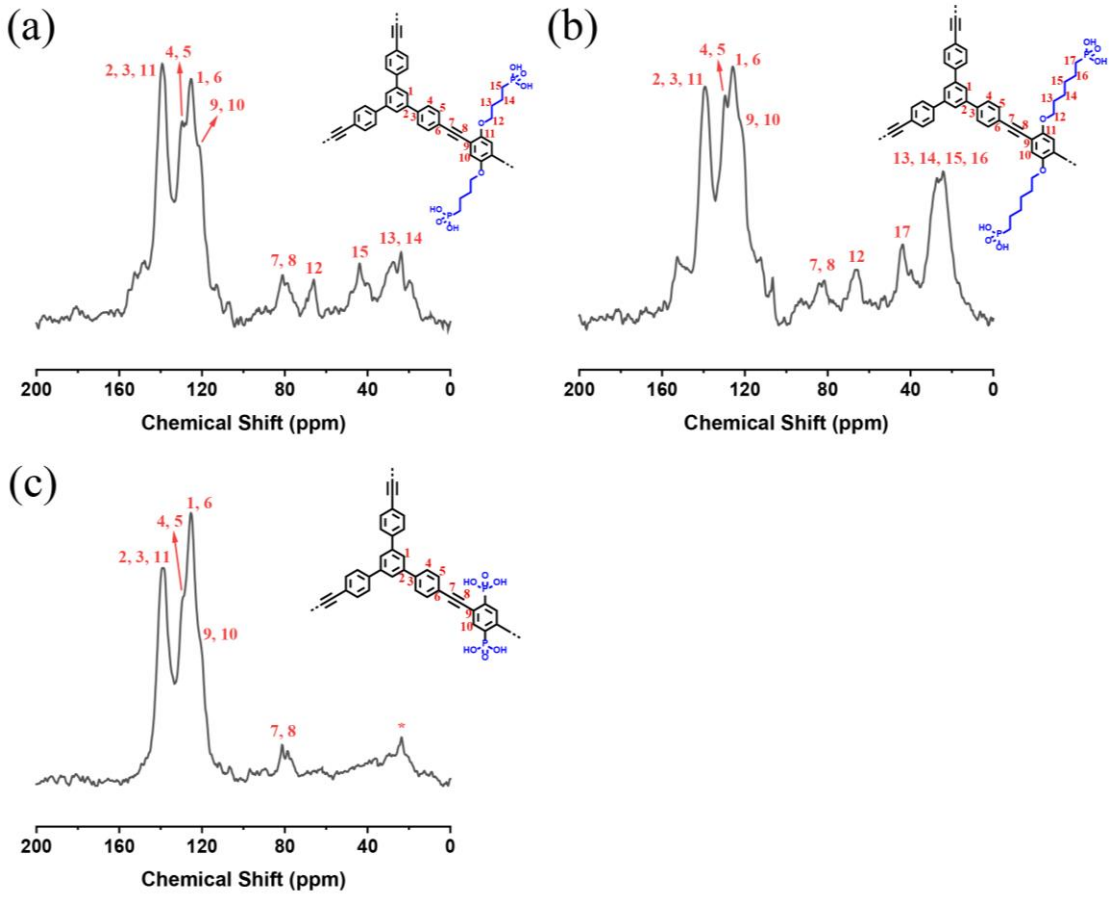

Figure S5. ^{13}C Solid-State NMR spectrum of CMP-**C4-P**, CMP-**C6-P**, and CMP-**P**. asterisk denote spinning sidebands.

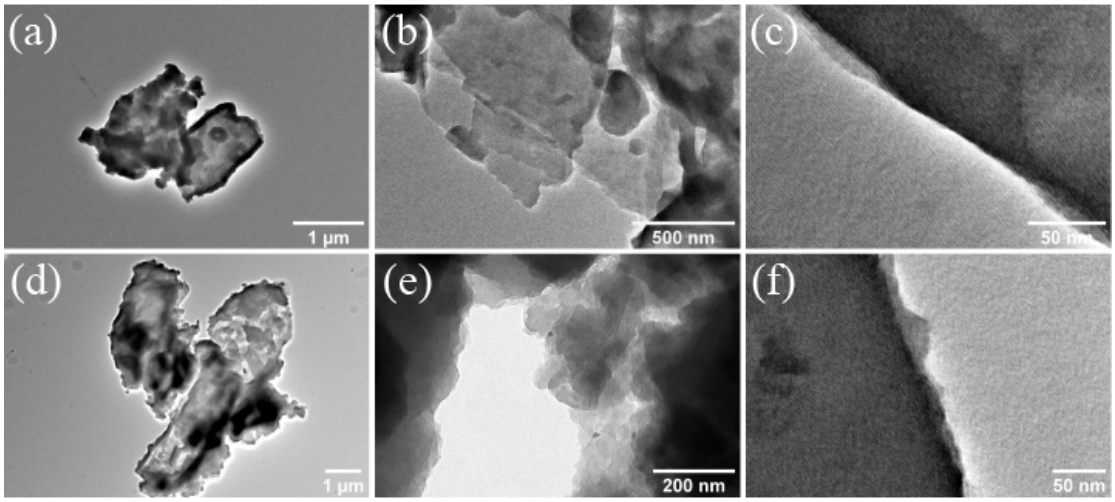

Figure S6. HR-TEM images of (a-c) **CMP-C2-P** and (d-f) CMP-**C2-P-45%**.

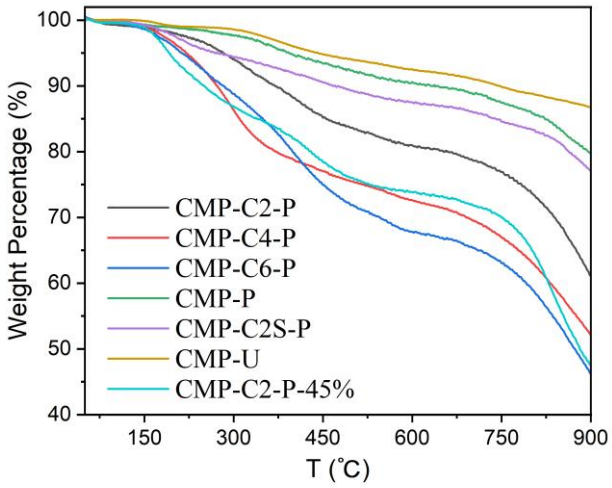

Figure S7. TGA curves of CMPs.

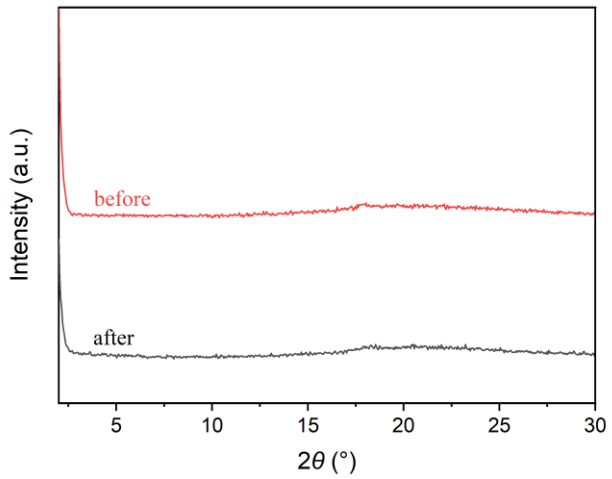

Figure S8. PXRD spectra of CMP-**C2-P** heat-treated at 155 °C for 12h.

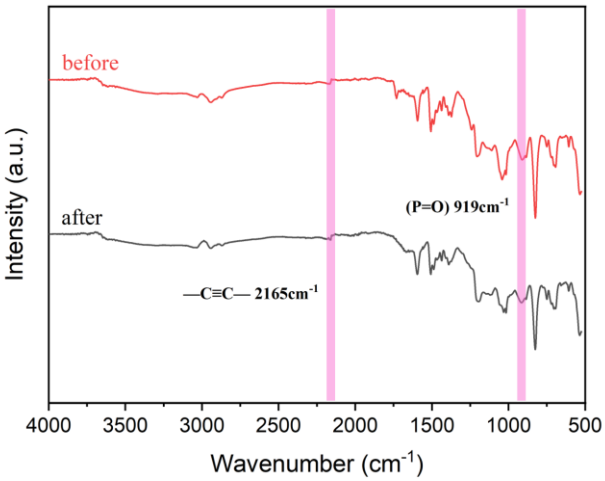

Figure S9. FT-IR spectra of CMP-**C2-P** heat-treated at 155 °C for 12h.

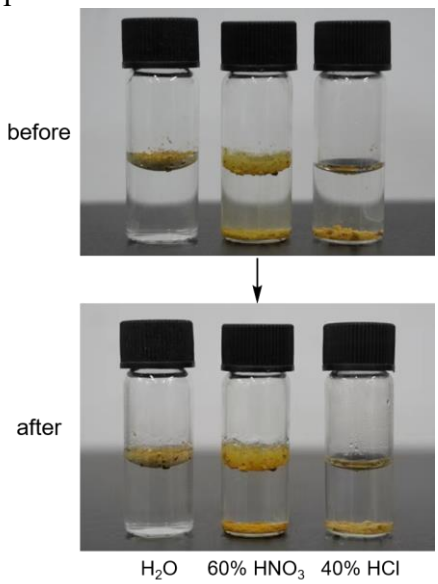

Figure S10. CMP-**C2-P** soaked in H_2O, 60% HNO_3, and 40% HCl for 24 h.

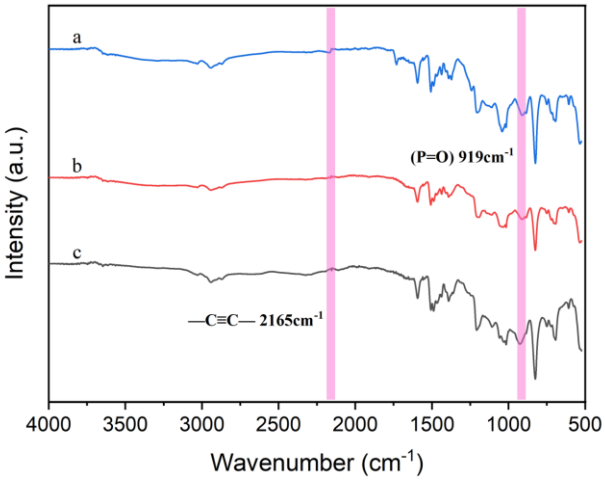

Figure S11. FT-IR spectra of CMP-**C2-P** soaked in (a) H_2O, (b) 60% HNO_3, and (c) 40% HCl for 24 h.

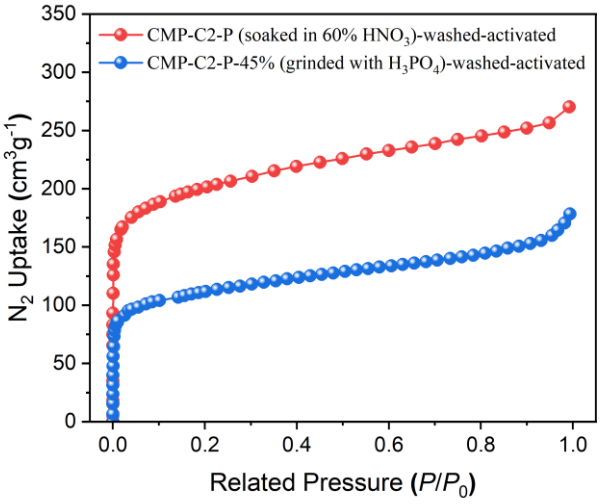

Figure S12. N_2 adsorption isotherms at 77 K of (a) CMP-**C2-P** soaked in 60% HNO_3 and (b) CMP-**C2-P-45%** after wash and activation.

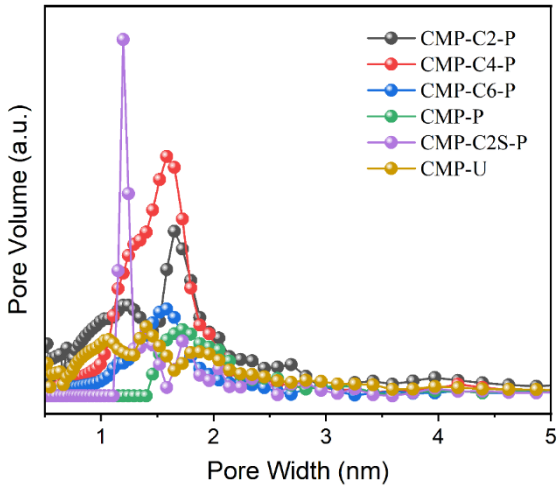

Figure S13. Pore size distribution of CMP**s**.

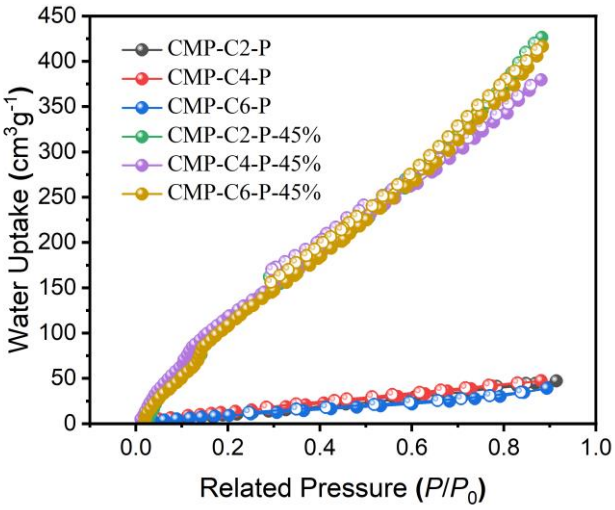

Figure S14. Water vapor adsorption isotherms of CMP-**C2/C4/C6-P** and CMP-**C2/C4/C6-P-45%**.

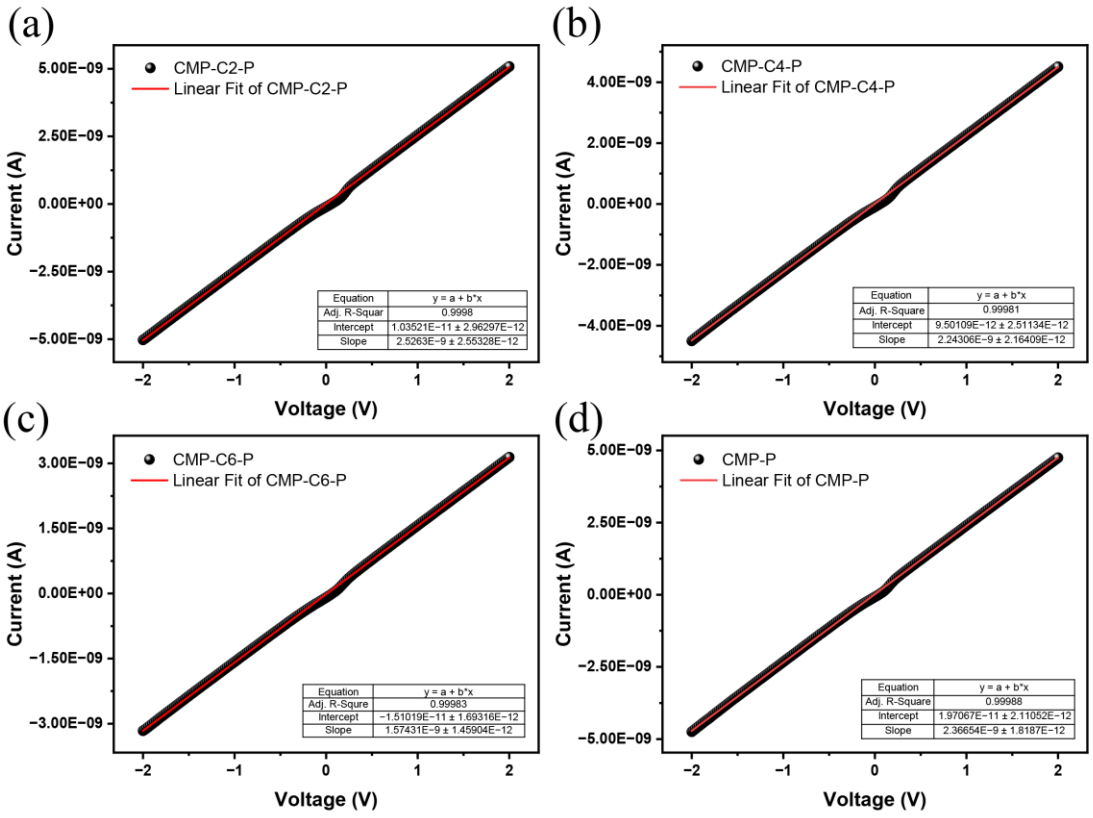

Figure S15. Current-voltage curves of CMP-**C2/C4/C6-P** and CMP-**P**.

The electronic conductivities of CMP-**C2/C4/C6-P** and CMP-**P** were calculated according to the equation:

$$\sigma = G\frac{L}{A}$$

Where electrical conductivity, σ, measures a material's ability to conduct electrical current. Measuring σ typically requires incorporating the material of interest into an electronic device, typically a resistor, and measuring the electrical conductance (G), length (L), and cross-sectional area (A) of the conduction channel.

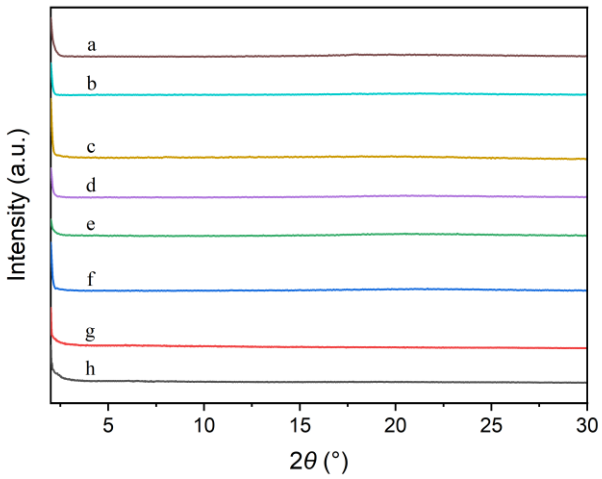

Figure S16. PXRD spectra of (a) CMP-**C2-P**, (b) CMP-**C2-P-45%**, (c) CMP-**C4-P**, (d) CMP-**C4-P-45%**, (e) CMP-**C6-P**, (f) CMP-**C6-P-45%**, (g) CMP-**P**, and (h) CMP-**P-45%**.

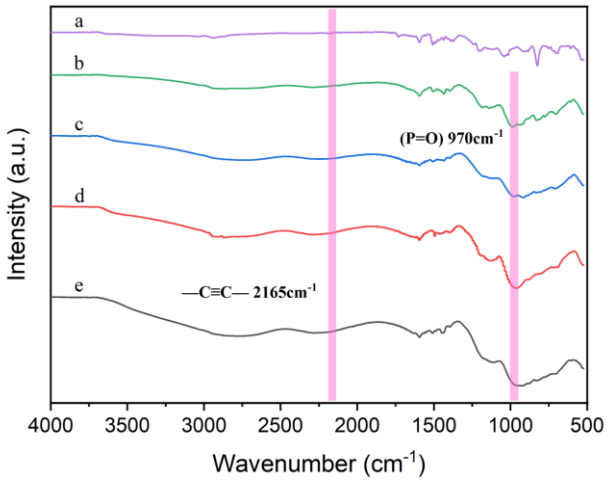

Figure S17. FT-IR spectra of (a) CMP-**C2-P**, (b) CMP-**C2-P-15%**, (c) CMP-**C2-P-30%**, (d) CMP-**C2-P-45%**, and (e) CMP-**C2-P-60%**.

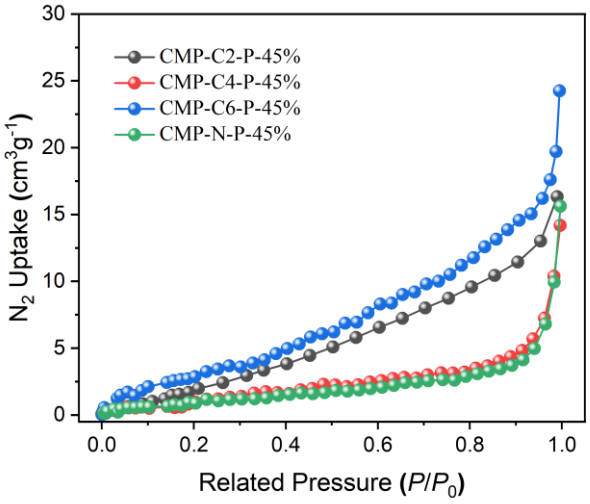

Figure S18. N_2 adsorption isotherms at 77 K of CMP-**C2**/**C4**/**C6-P** and CMP-**P**.

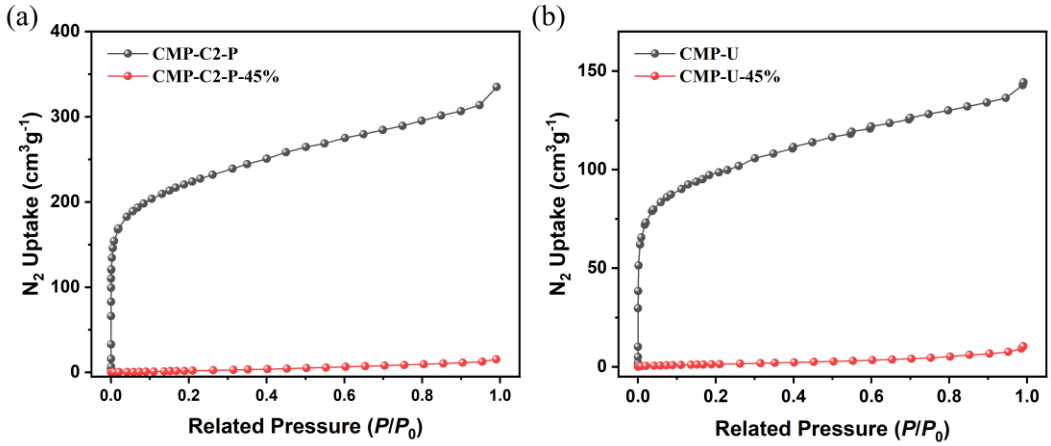

Figure S19. N_2 adsorption isotherms at 77 K of (a) CMP-**C2-P** and CMP-**C2-P-45%** and (b) CMP-**U**, and CMP-**U-45%**.

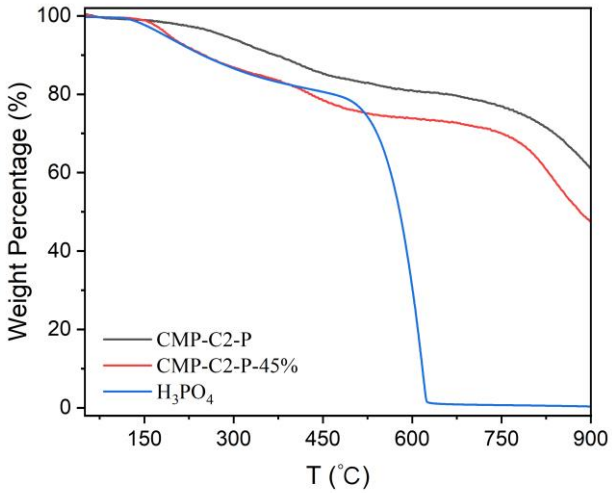

Figure S20. TGA curves of CMP-**C2-P**, CMP-**C2-P-45%**, and H_3PO_4.

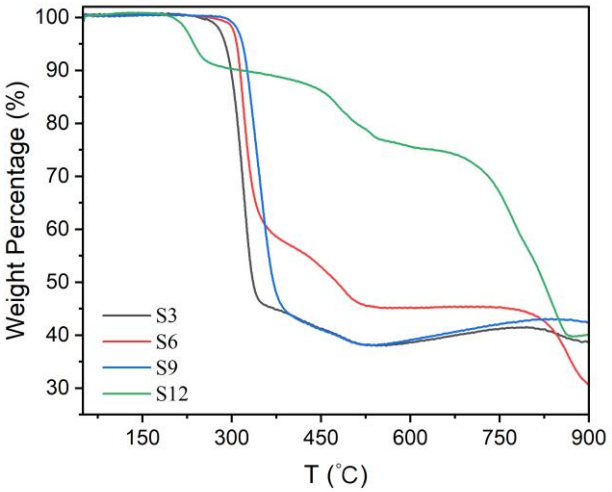

Figure S21. TGA curves of **S3**, **S6**, **S9**, and **S12**.

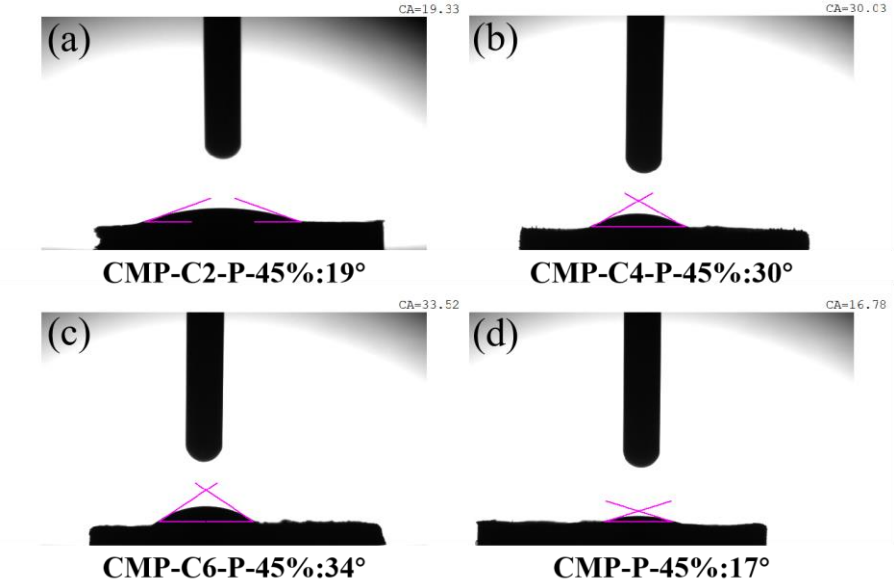

Figure S22. Water contact angles of CMP-**C2/C4/C6-P-45%** and CMP-**P-45%**.

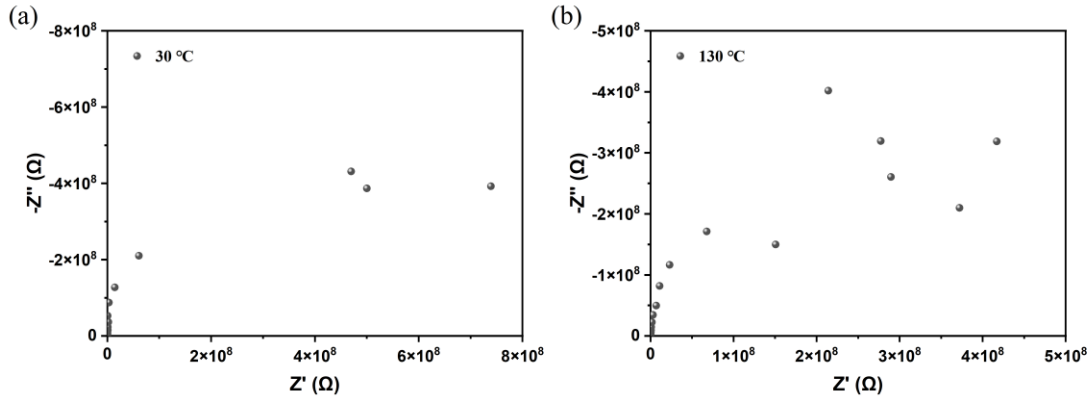

Figure S23. Nyquist plots of CMP-**C2-P** measured at 30 and 130°C under anhydrous conditions.

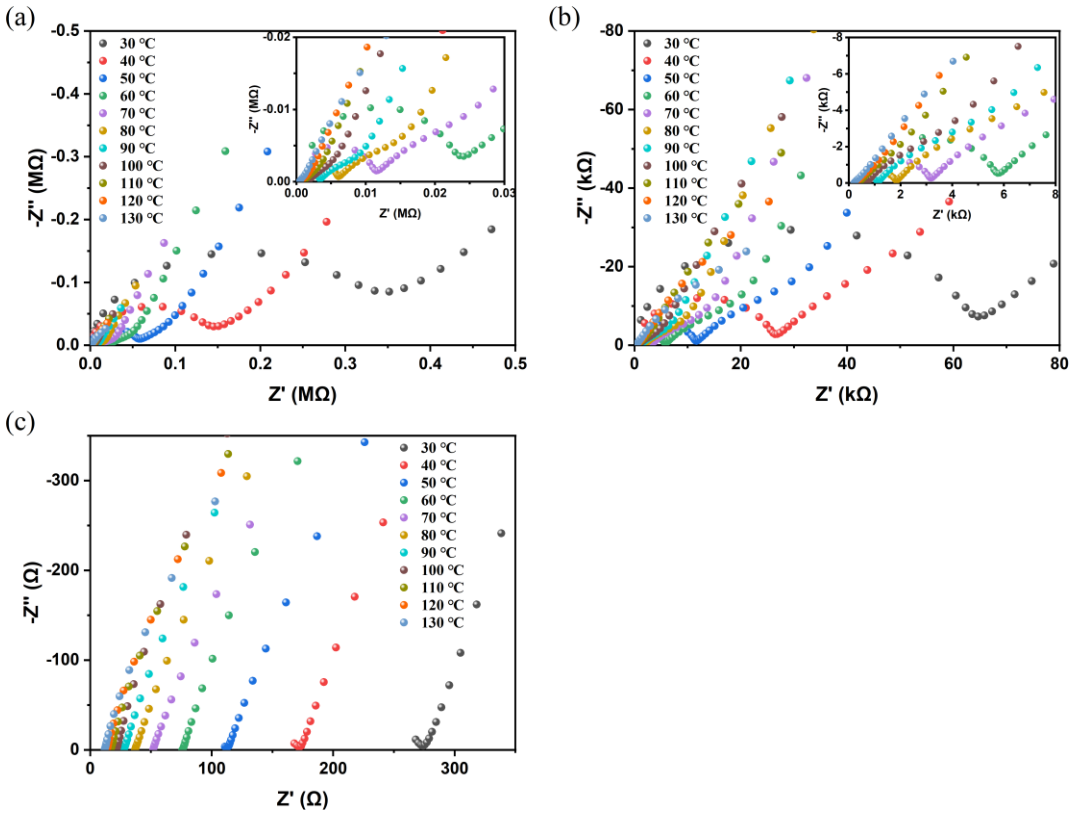

Figure S24. Nyquist plots of (a) CMP-**C2-P-15%**, (b) CMP-**C2-P-30%**, and (c) CMP-**C2-P-60%** measured at 30~130°C under anhydrous conditions.

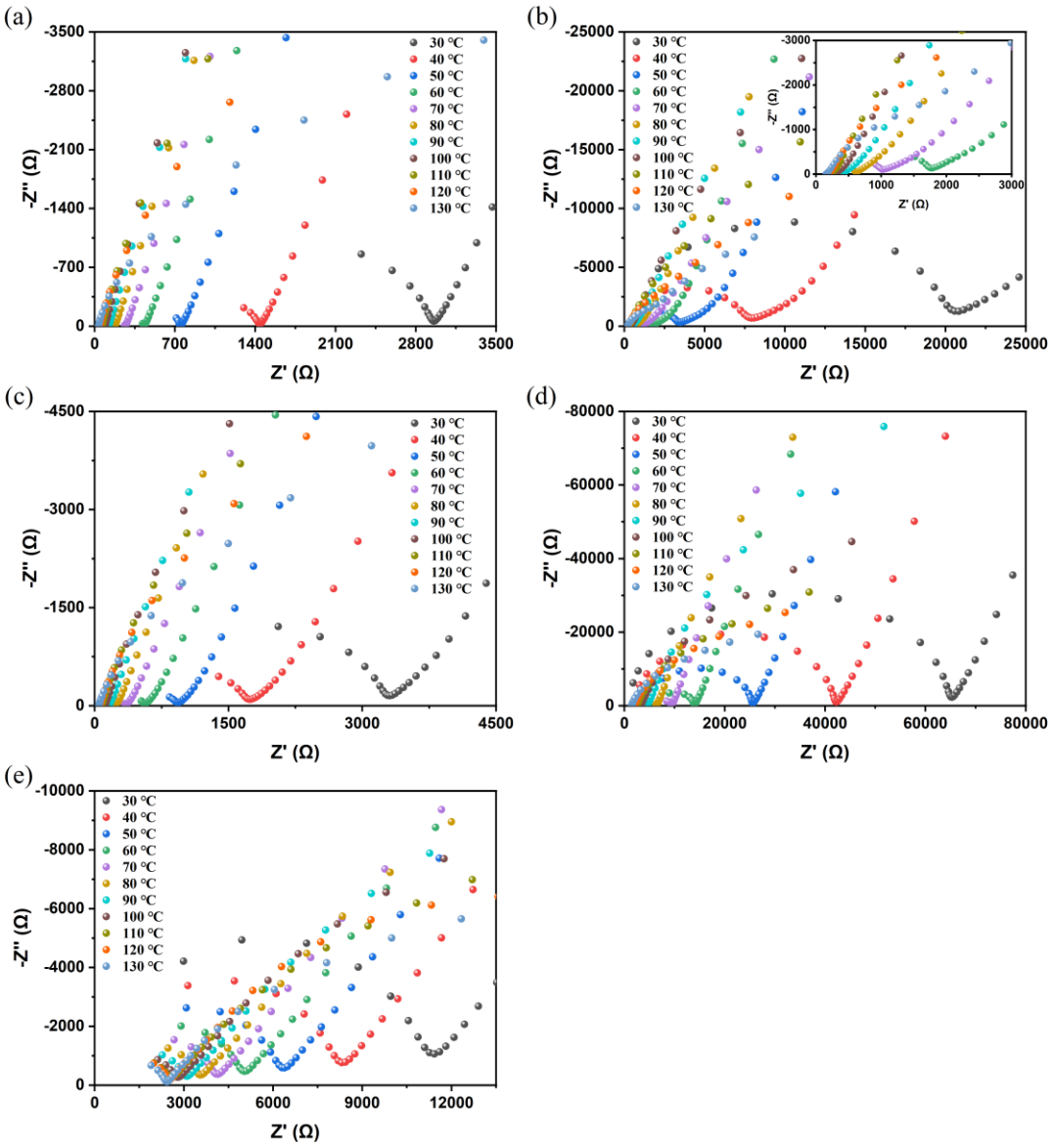

Figure S25. Nyquist plots of (a) CMP-**C4-P-45%**, (b) CMP-**C6-P-45%**, (c) CMP-**P-45%**, (d) CMP-**C2S-P-45%**, and (e) CMP-**U-45%** measured at 30~130°C under anhydrous conditions.

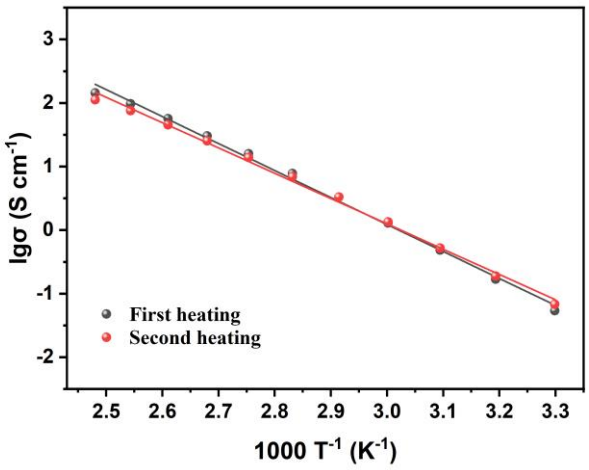

Figure S26. Cycling test for CMP-**C2-P-45%** at 30~130°C under anhydrous conditions.

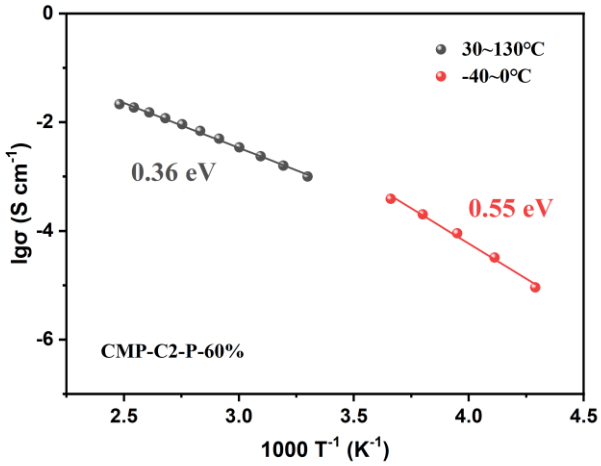

Figure S27. Arrhenius plots for CMP-**C2-P-60%** at –40~130 °C under anhydrous conditions.

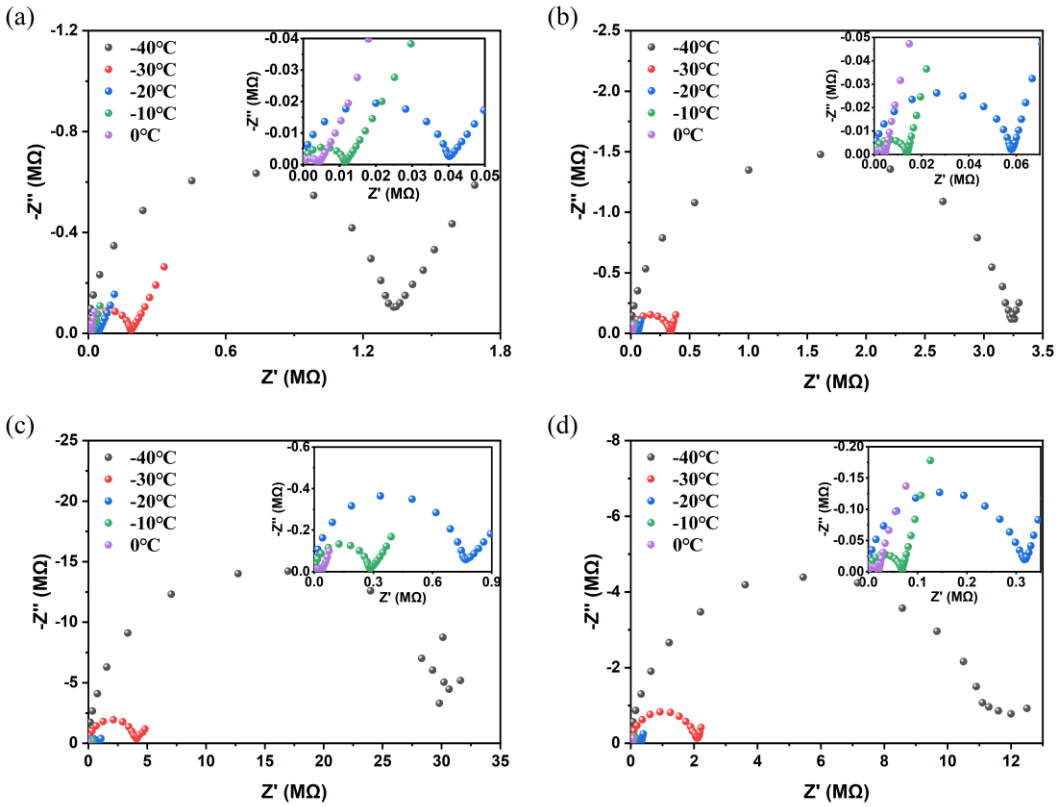

Figure S28. Nyquist plots of (a) CMP-**C2-P-45%**, (b) CMP-**C4-P-45%**, (c) CMP-**C6-P-45%**, and (d) CMP-**P-45%** measured at –40~0 °C under anhydrous conditions.

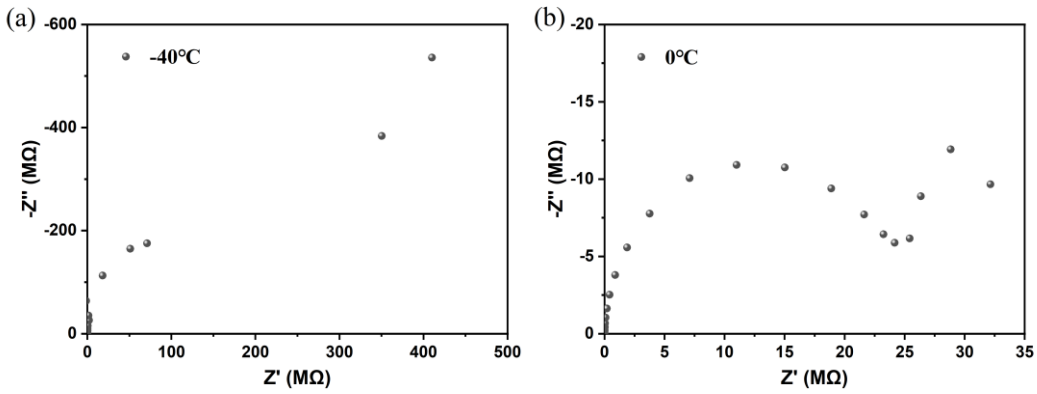

Figure S29. Nyquist plots of H_3PO_4@CMP-F6-45% measured at –40 and 0 °C under anhydrous conditions.

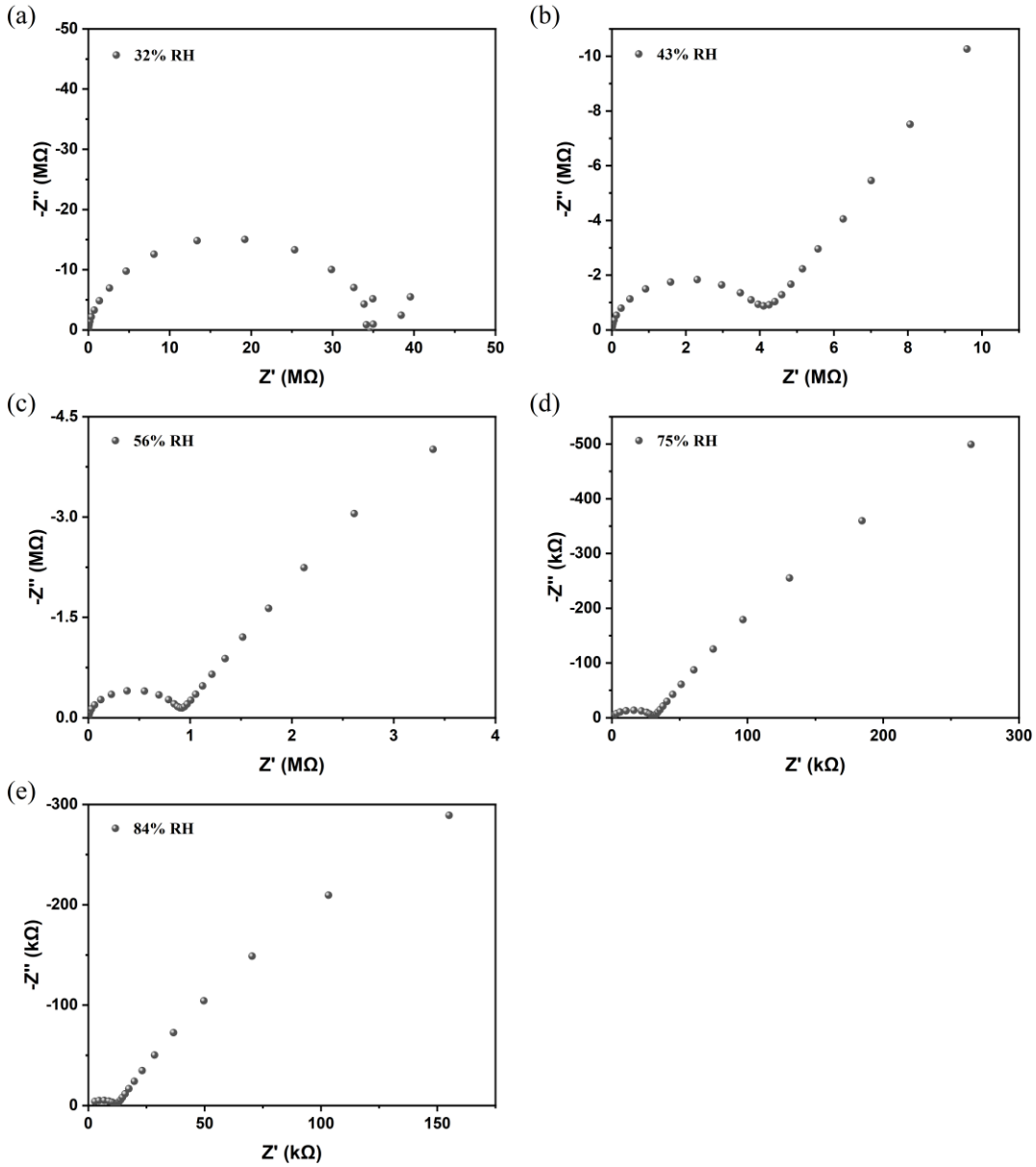

Figure S30. Nyquist plots of CMP-**C2-P** under (a) 32%, (b) 43%, (c) 56%, (d) 75%, and (e) 84% RH at 30 °C.

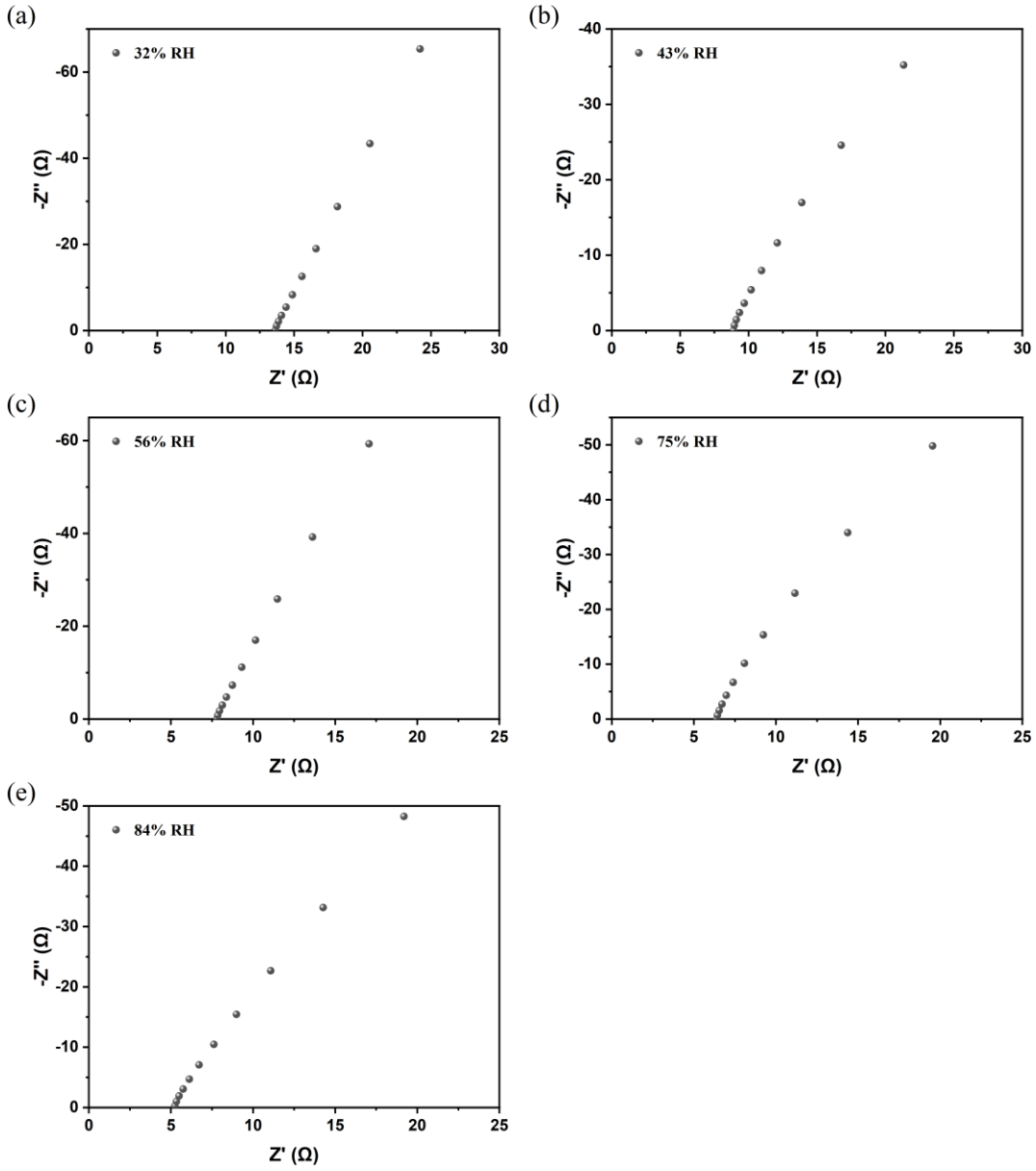

Figure S31. Nyquist plots of CMP-**C2-P-45%** under (a) 32%, (b) 43%, (c) 56%, (d) 75%, and (e) 84% RH at 30 °C.

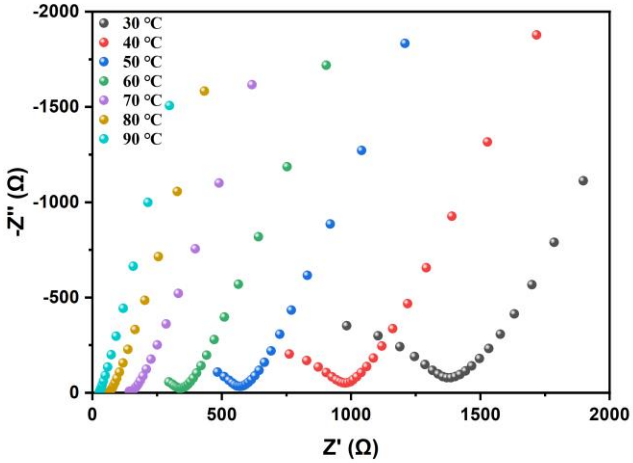

Figure S32. Nyquist plots of CMP-**C2-P** under 98% RH at 30~90°C.

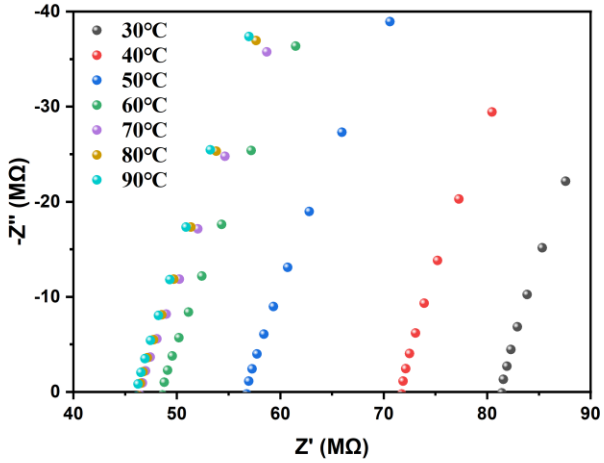

Figure S33. Nyquist plots of H_3PO_4@CMP-F6-45% under 98% RH at 30~90°C.

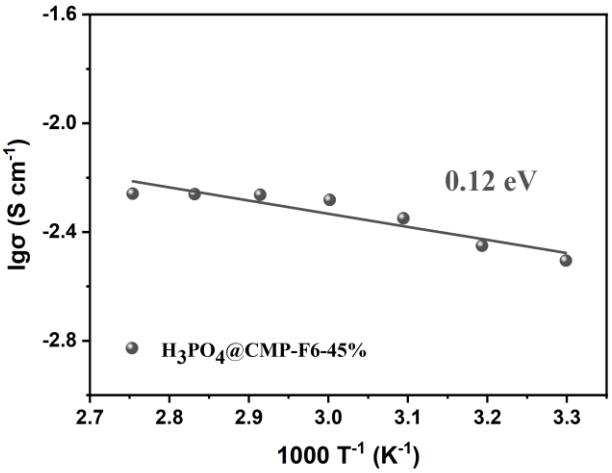

Figure S34. Arrhenius plots of H_3PO_4@CMP-F6-45% under 98% RH.

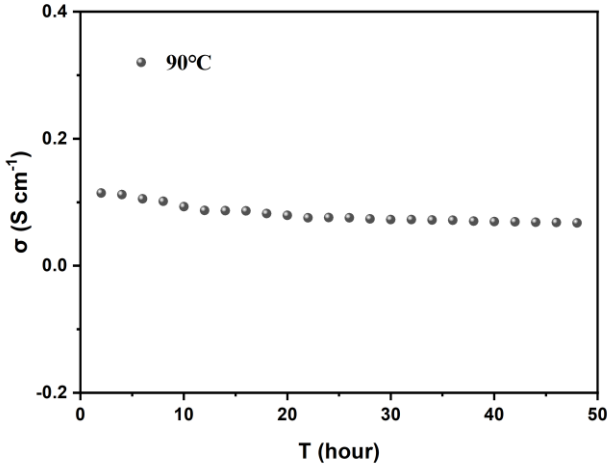

Figure S35. Long-period test for CMP-**C2-P-45%** under 98% RH at 90℃.

Table S36. Comparison of proton conductivities in reported materials.

Material	Type	Proton conductivity (S cm^{-1})	Condition	Temperature (℃)	Reference
CMP-**C2-P-H**	pellet	2.15×10^{-2}	anhydrous	130	This work
PA@Tp-Azo	pellet	6.70×10^{-5}	anhydrous	67	J. Am. Chem. Soc. 2014, 136, 6570−6573.
Im@Td-PPI	pellet	3.49×10^{-4}	anhydrous	90	J. Am. Chem. Soc. 2015, 137, 913−918.
Im@Td-PNDI	pellet	9.04×10^{-5}	anhydrous	90	J. Am. Chem. Soc. 2015, 137, 913−918.
PA@TpBpy-ST	pellet	1.98×10^{-3}	anhydrous	120	J. Mater. Chem. A, 2016, 4, 2682−2690.
PA@TpBpy-MC	pellet	2.50×10^{-3}	anhydrous	120	J. Mater. Chem. A, 2016, 4, 2682−2690.
TpPa-SO_3H	pellet	1.70×10^{-5}	anhydrous	120	Chem. Mater. 2016, 28, 1489−1494.
Phytic acid@TpPa-(SO_3H-Py)	pellet	5.00×10^{-4}	anhydrous	120	Chem. Mater. 2016, 28, 1489−1494.
Im@TPB-DMTP-COF	pellet	4.37×10^{-3}	anhydrous	130	Nat. Mater. 2016, 15, 722−726.
Tri@TPB-DMTP-COF	pellet	1.10×10^{-3}	anhydrous	130	Nat. Mater. 2016, 15, 722−726.
HL@0.202Him	pellet	6.57×10^{-5}	anhydrous	120	Chem. Commun. 2017, 53, 2475−2478.
PA@EB-COF	pellet	5.88×10^{-3}	anhydrous	130	J. Mater. Chem. A, 2020, 8, 13702−13709.
Tra@EB-COF	pellet	2.31×10^{-3}	anhydrous	130	J. Mater. Chem. A, 2020, 8, 13702−13709.
Im@Py-TT-COF-50	pellet	3.08×10^{-3}	anhydrous	130	ACS Appl. Mater. Interfaces, 2020, 12, 22910−22916.
H_3PO_4@TPB-DMeTP-COF	pellet	1.91×10^{-1}	anhydrous	160	Nat. Commun. 2020, 11, 1981.
COF-F6-H	pellet	4.20×10^{-2}	anhydrous	140	J. Am. Chem. Soc. 2020, 142, 14357−14364.
H_3PO_4@CMP-F6-60%	pellet	4.39×10^{-3}	anhydrous	120	ACS Appl. Mater. Interfaces, 2021, 13, 15536−15541.
F6-[dema]HSO_4-1.5	pellet	1.33×10^{-2}	anhydrous	140	ACS Appl. Mater. Interfaces, 2021, 13, 37172−37178.
H_3PO_4@TPB-DABI-COF (66 wt%)	pellet	1.52×10^{-1}	anhydrous	160	Angew. Chem. Int. Ed. 2021, 60,

					12918−12923.
PIL-TB-COF	pellet	1.52×10^{-4}	anhydrous	120	J. Mater. Chem. A, 2022, 10, 6499−6507.
CTF-Mx	mambrane	2.08×10^{-2}	anhydrous	160	ACS Appl. Mater. Interfaces, 2021, 13, 13604−13612.
MPOPS-1	membrane	1.49×10^{-5}	anhydrous	77	ACS Sustainable Chem. Eng. 2020, 8, 2423−2432.
H@TPT-COF	pellet	1.27×10^{-2}	anhydrous	160	Angew. Chem. Int. Ed. 2022, e202208086.
CMP-**C2-P-H**	pellet	1.15×10^{-5}	anhydrous	–40	This work
Im@Td-PNDI	pellet	4.58×10^{-7}	anhydrous	–40	J. Am. Chem. Soc. 2015, 137, 913−918.
Im@Td-PPI	pellet	2.23×10^{-6}	anhydrous	–40	J. Am. Chem. Soc. 2015, 137, 913−918.
HCl⊂1	pellet	5.00×10^{-7}	anhydrous	–40	Adv. Mater. 2016, 28, 1663−1667.
FJU-31@Ch	pellet	1.17×10^{-6}	anhydrous	–40	J. Mater. Chem. A, 2016, 4, 4062−4070.
FJU-31@Hq	pellet	3.24×10^{-6}	anhydrous	–40	J. Mater. Chem. A, 2016, 4, 4062−4070.
PA@TpBpy-ST	membrane	1.53×10^{-4}	anhydrous	–40	J. Mater. Chem. A, 2016, 4, 2682−2690.
PA@TpBpy-MC	membrane	1.92×10^{-4}	anhydrous	–40	J. Mater. Chem. A, 2016, 4, 2682−2690.
CMP-**C2-P-H**	pellet	9.93×10^{-2}	98% RH	90	This work
PA@Tp-Stb	pellet	2.30×10^{-5}	98% RH	59	J. Am. Chem. Soc. 2014, 136, 6570−6573.
PA@Tp-Azo	pellet	9.90×10^{-4}	98% RH	59	J. Am. Chem. Soc. 2014, 136, 6570−6573.
NUS-9(R)	pellet	1.24×10^{-2}	97% RH	25	ACS Appl. Mater. Interfaces, 2016, 8, 18505−18512.
NUS-10(R)	pellet	3.96×10^{-2}	97% RH	25	ACS Appl. Mater. Interfaces, 2016, 8, 18505−18512.
EB-COF-Br	pellet	2.82×10^{-5}	97% RH	25	J. Am. Chem. Soc. 2016, 138, 5897−5903.
EB-COF:PW_{12}	pellet	3.32×10^{-3}	97% RH	20	J. Am. Chem. Soc. 2016, 138, 5897−5903.
LiCl@RT-COF-1	membrane	6.45×10^{-3}	100% RH	40	J. Am. Chem. Soc. 2017, 139, 10079−10086.
PTSA@TpAzo	membrane	7.80×10^{-2}	95% RH	80	Angew. Chem. Int. Ed. 2018,

					57, 10894−10898.
BIP	pellet	3.20×10^{-2}	95% RH	95	J. Am. Chem. Soc. 2019, 141, 14950−14954.
aza-COF-2H	pellet	4.80×10^{-3}	97% RH	50	Chem. Mater. 2019, 31, 819−825.
H_3PO_4@NKCOFs	membrane	1.13×10^{-1}	98% RH	80	Angew. Chem. Int. Ed. 2020, 59, 3678−3684.
H_3PO_4@NKCOF-10	membrane	9.04×10^{-2}	90% RH	80	Nat. Commun. 2021, 12, 1982.
PEEK@Ox-DBD-COF-SO_3H	pellet	3.87×10^{-3}	98% RH	90	Chem. Eur. J. 2021, 27, 3817−3822.
MPOPS-1	membrane	3.07×10^{-2}	98% RH	77	ACS Sustainable Chem. Eng. 2020, 8, 2423−2432.
SA@H_8L-Ni-Crystal	membrane	5.28×10^{-2}	98% RH	90	Chem. Asian J. 2021, 16, 1562–1569.
Uio-66(SO_3H)$_2$	pellet	8.40×10^{-2}	90% RH	80	Angew. Chem. Int. Ed. 2015,54, 5142–5146.
Im@(NENU-3)	pellet	1.82×10^{-2}	90% RH	70	J. Am. Chem. Soc. 2017, 139, 15604−15607.
MROF-1	pellet	1.72×10^{-2}	97% RH	70	J. Mater. Chem. A, 2016, 4, 18742–18746.
HOFs	membrane	1.80×10^{-2}	90% RH	80	J. Mater. Chem. A, 2017, 5, 17492–17498.
CPOS-1	membrane	1.00×10^{-2}	98% RH	60	J. Mater. Chem. A, 2020, 8, 7474–7494.
PAPOP-DD-0.5	pellet	7.09×10^{-2}	98% RH	75	Ind. Eng. Chem. Res. 2021, 60, 6337−6343.
SBO-CMP-2	pellet	5.21×10^{-2}	100% RH	70	Langmuir, 2018, 34, 7640−7646.
1S	pellet	7.72×10^{-2}	90% RH	80	Angew. Chem. Int. Ed. 2016, 55, 16123–16126.
1ES	pellet	1.59×10^{-1}	90% RH	80	J. Mater. Chem. A, 2017, 5, 17492–17498.
S-POPs	pellet	1.00×10^{-1}	95% RH	80	Mater. Chem. Front. 2020, 4, 2339–2345.
SPAF-1	pellet	1.60×10^{-1}	95% RH	80	Chem. Commun. 2017, 53, 7592-7595.
IL-COF-SO_3H@SNF-35	composite membrane	2.24×10^{-1}	100% RH	90	Chem. Eng. J. 2021, 514, 129021.
HPW@COF/SPEEK	composite membrane	2.80×10^{-1}	100% RH	75	Solid State Ionics, 2020, 349, 115316.
COF-1-Li@M	composite	1.30×10^{-1}	98% RH	40	ACS Appl.

	membrane				Mater. Interfaces, 2020, 12, 8198−8205.

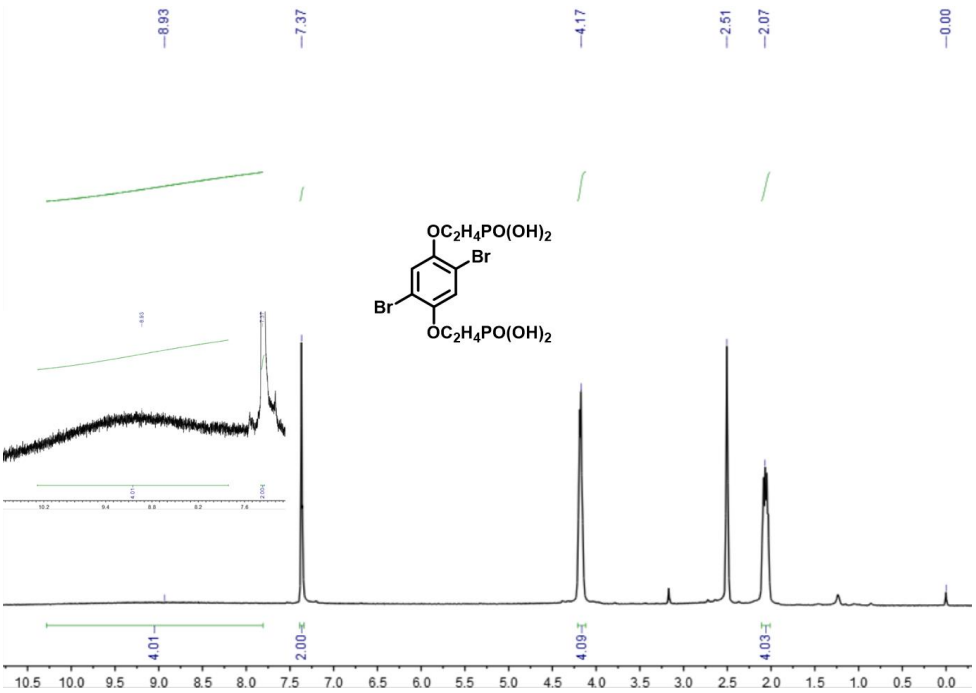
8.93
7.37
4.17
2.51
2.07
0.00
OC2H4PO(OH)2
Br
Br
OC2H4PO(OH)2
4.01
2.00
4.09
4.03

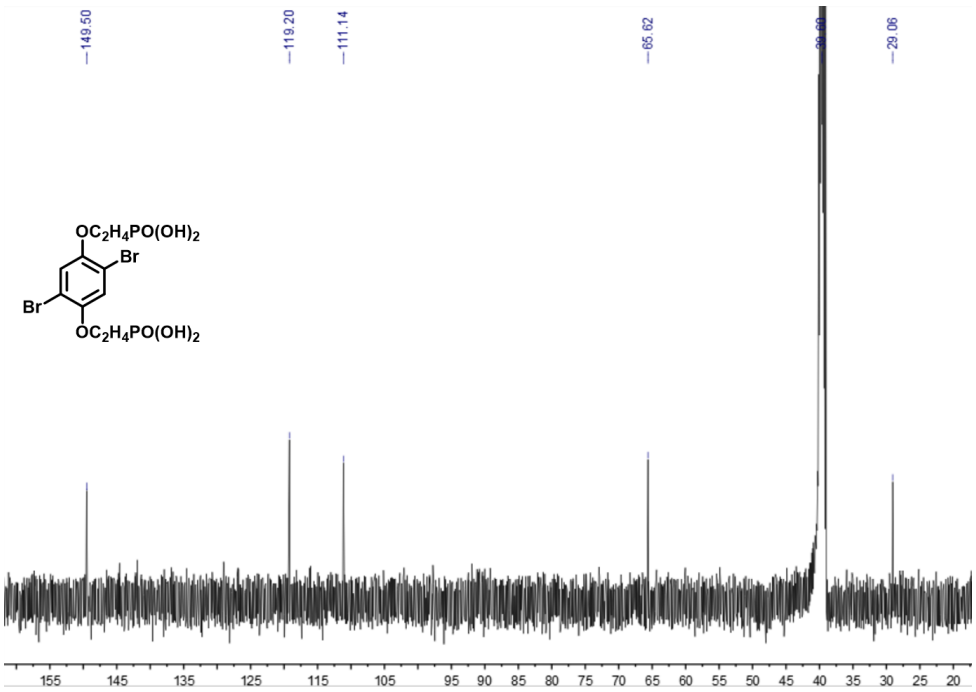
149.50
119.20
111.14
65.62
29.06
OC2H4PO(OH)2
Br
Br
OC2H4PO(OH)2

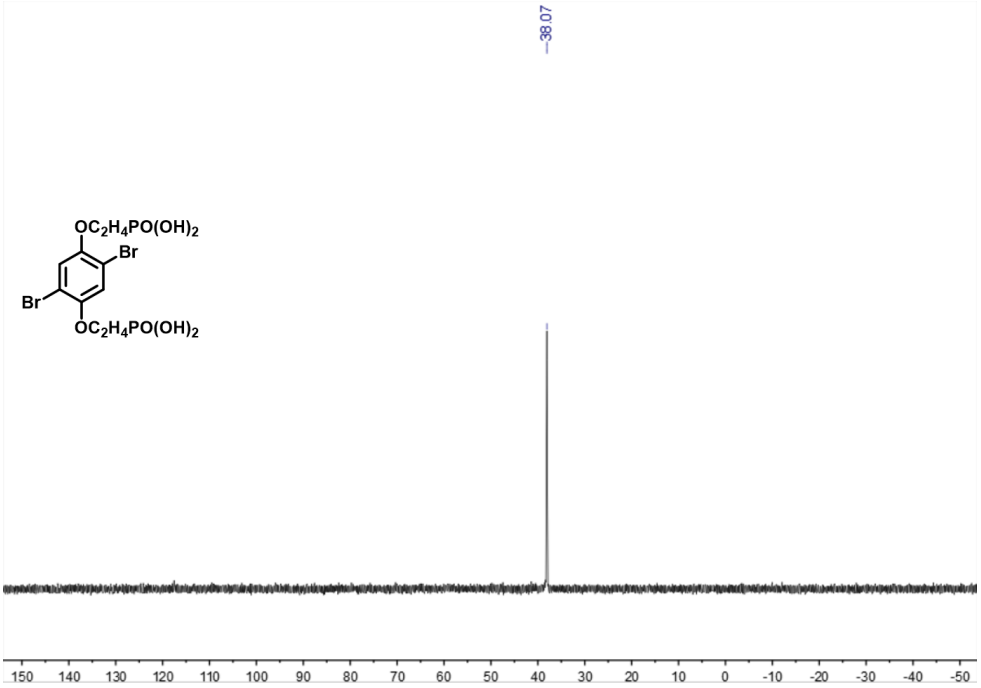

Figure S37. ^{1}H, ^{13}C and ^{31}P NMR Liquid-State NMR spectrum of **S3**.

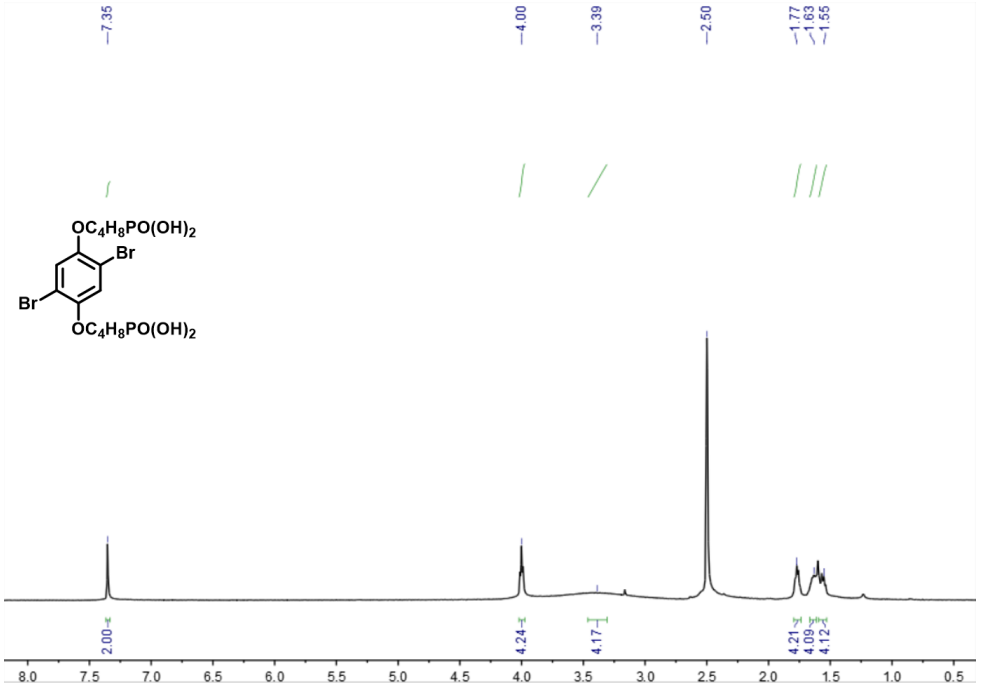

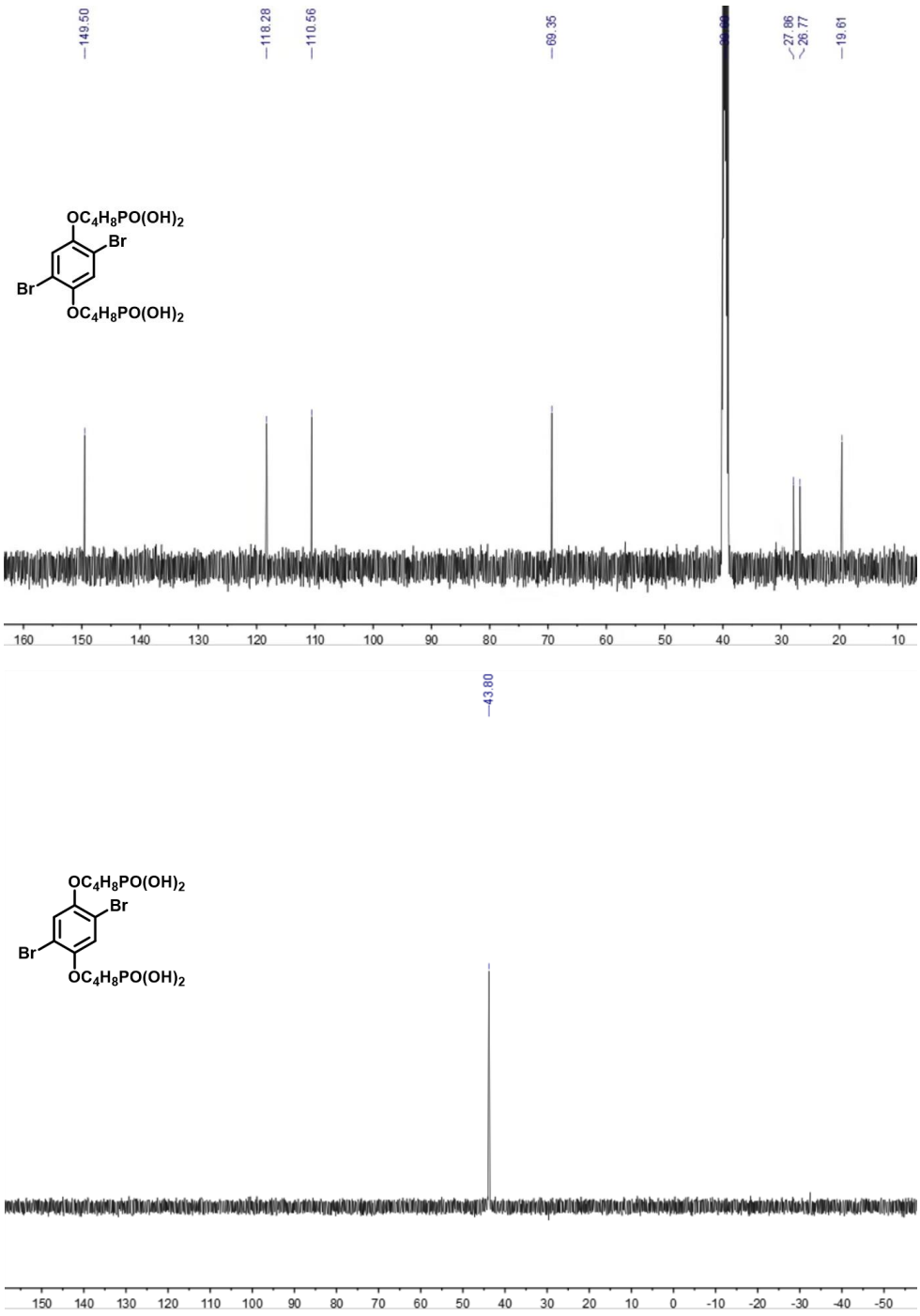

Figure S38. ^{1}H, ^{13}C and ^{31}P NMR Liquid-State NMR spectrum of **S6**.

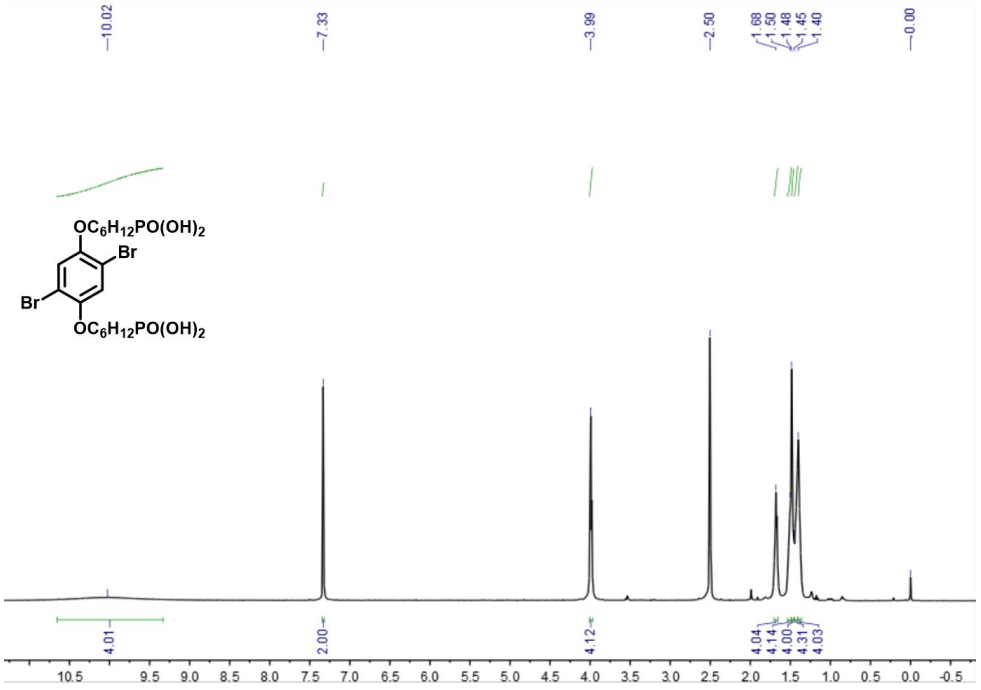
10.02
7.33
3.99
2.50
1.68
1.50
1.48
1.45
1.40
0.00
OC6H12PO(OH)2
Br
Br
OC6H12PO(OH)2
4.01
2.00
4.12
4.04
4.14
4.00
4.31
4.03
10.5 9.5 9.0 8.5 8.0 7.5 7.0 6.5 6.0 5.5 5.0 4.5 4.0 3.5 3.0 2.5 2.0 1.5 1.0 0.5 0.0 -0.5

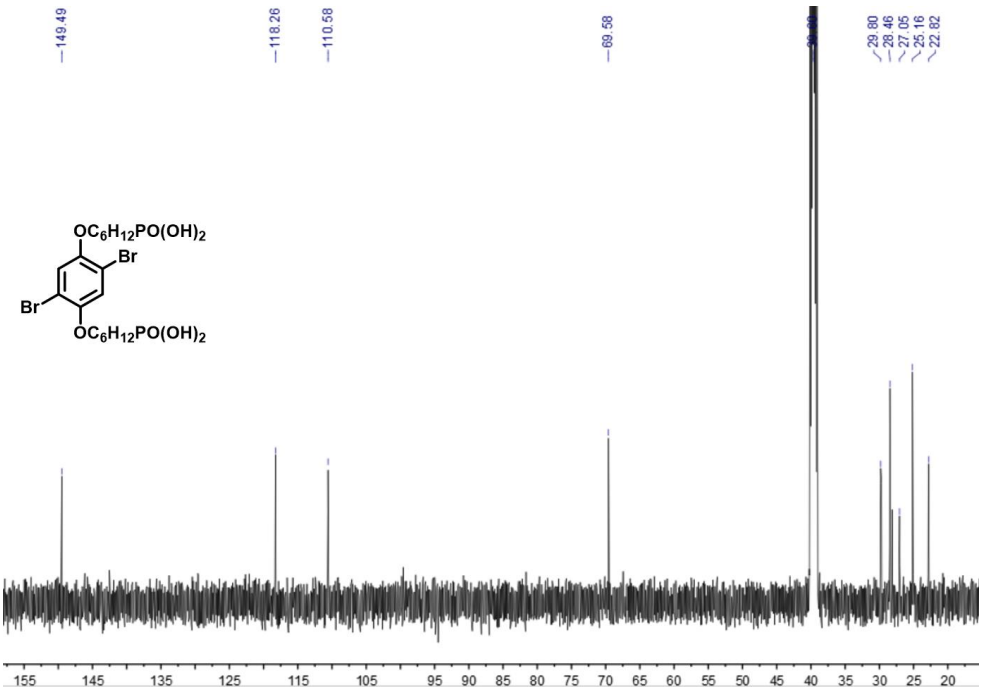
149.49
118.26
110.58
69.58
29.80
28.46
27.05
25.16
22.82
OC6H12PO(OH)2
Br
Br
OC6H12PO(OH)2
155 145 135 125 115 105 95 90 85 80 75 70 65 60 55 50 45 40 35 30 25 20

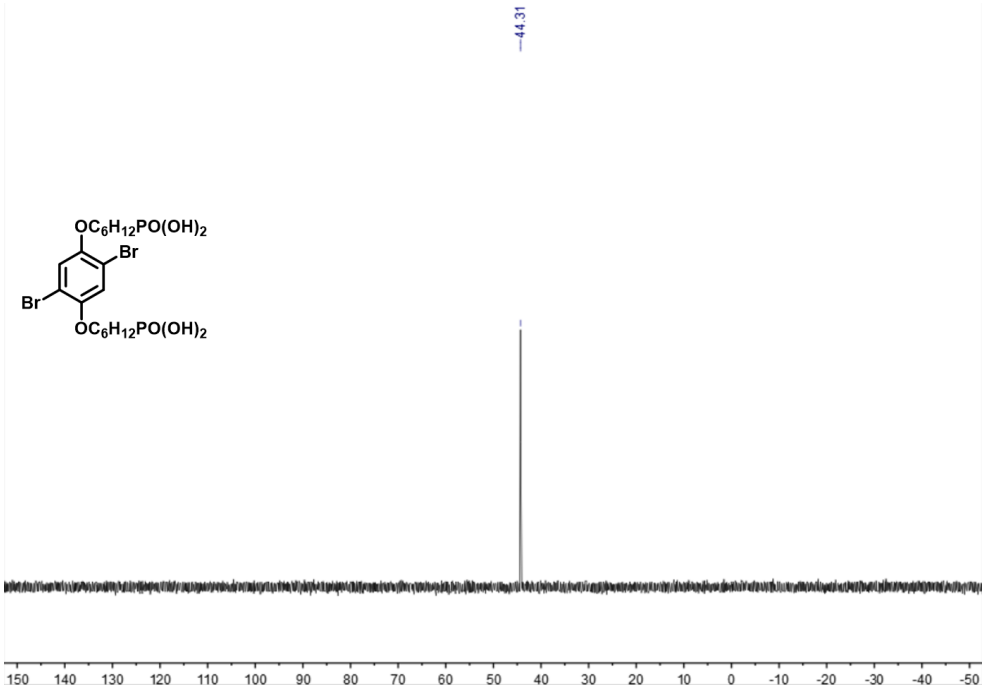

Figure S39. ^{1}H, ^{13}C and ^{31}P NMR Liquid-State NMR spectrum of **S9**.

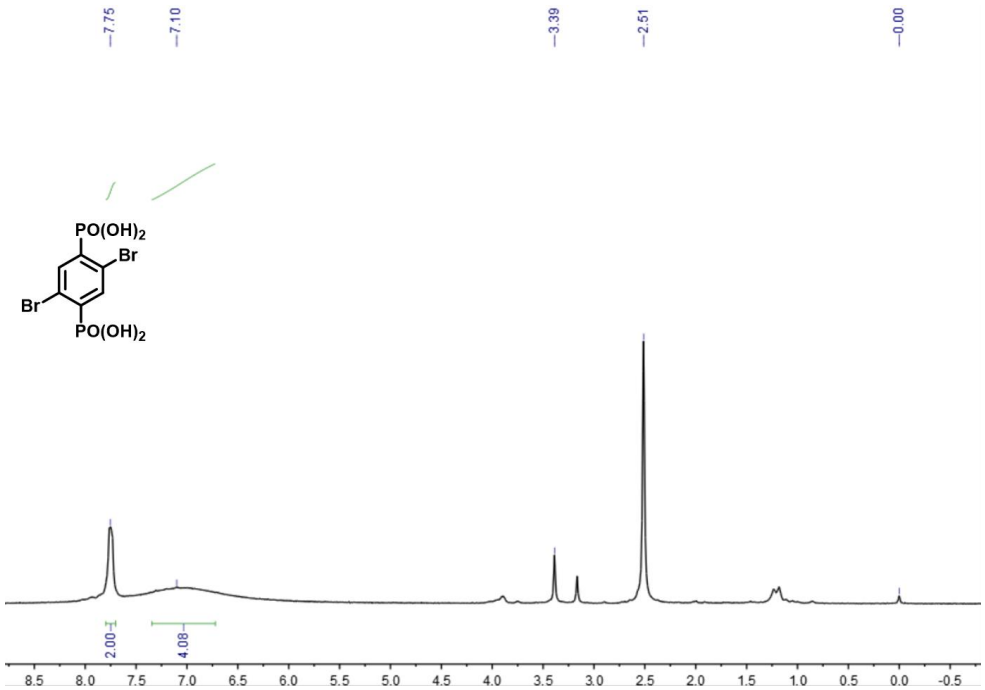

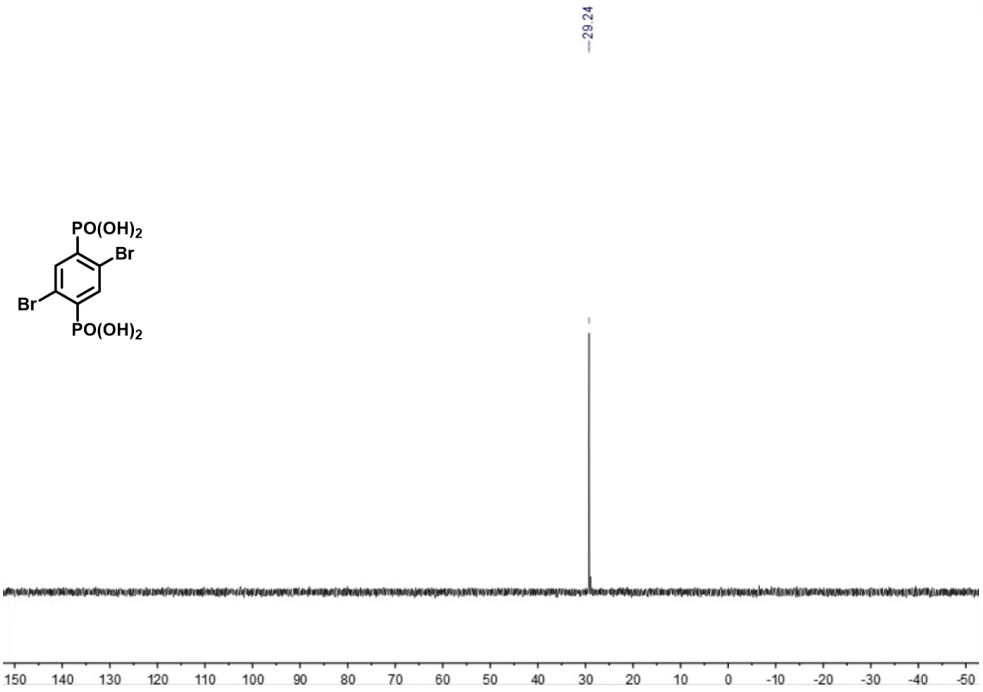

Figure S40. ^{1}H and ^{31}P NMR Liquid-State NMR spectrum of **S12**.

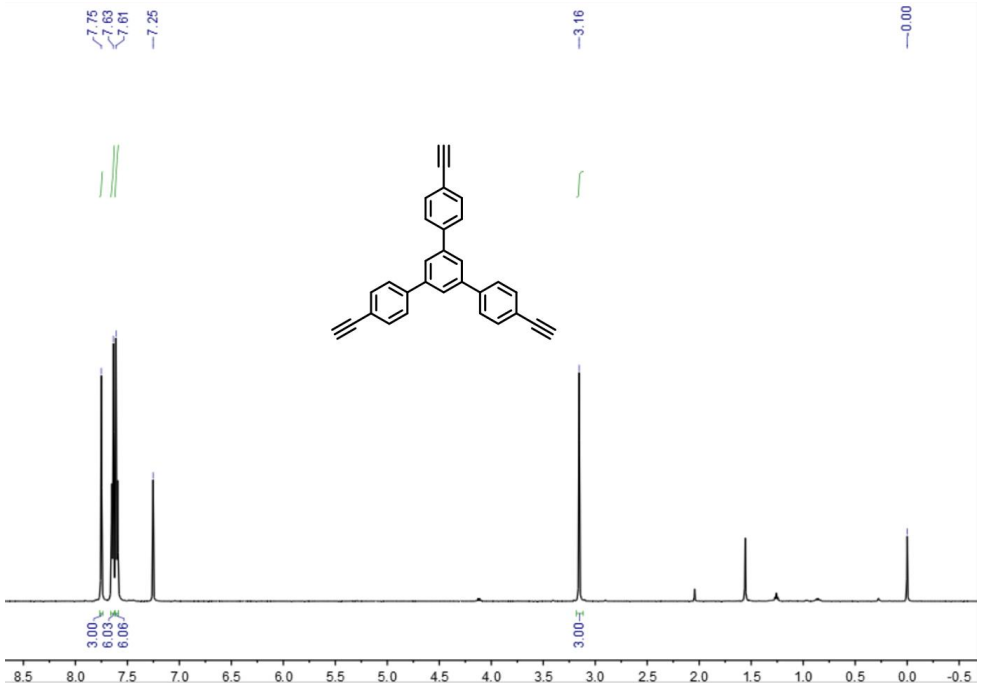

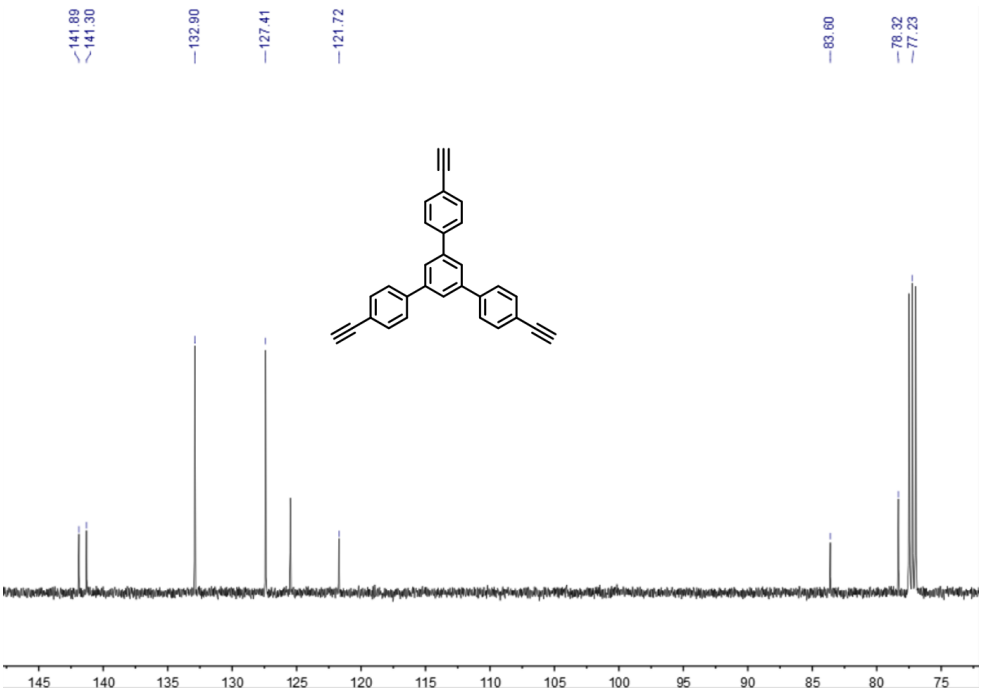

Figure S41. ^{1}H and ^{13}C NMR Liquid-State NMR spectrum of 1,3,5-triethynyltriphenylbenzene.

4. References

1. Guo LX, Wang HP, Wang YX, Liu F, Feng LH. Organic polymer nanoparticles with primary ammonium salt as potent antibacterial nanomaterials. ACS Appl Mater Interfaces. **12**(19), 21254-21262 (2020). doi:10.1021/acsami.9b19921
2. Hermer N, Stock N. The new triazine-based porous copper phosphonate cu-3(ppt)(h2o)(3) center dot 10h(2)o. Dalton Trans. **44**(8), 3720-3723 (2015). doi:10.1039/c4dt03698k
3. Jiang J-X, Su F, Trewin A, Wood CD, Campbell NL, Niu H, Dickinson C, Ganin AY, Rosseinsky MJ, Khimyak YZ, Cooper AI. Conjugated microporous poly (aryleneethynylene) networks. Angew Chem Int Ed. **46**(45), 8574-8578 (2007). doi:10.1002/anie.200701595
4. Dawson R, Laybourn A, Clowes R, Khimyak YZ, Adams DJ, Cooper AI. Functionalized conjugated microporous polymers. Macromolecules. **42**(22), 8809-8816 (2009). doi:10.1021/ma901801s
5. Zhang P, Weng ZH, Guo J, Wang CC. Solution-dispersible, colloidal, conjugated porous polymer networks with entrapped palladium nanocrystals for heterogeneous catalysis of the suzuki-miyaura coupling reaction. Chem Mater. **23**(23), 5243-5249 (2011). doi:10.1021/cm202283z
6. Lee J-SM, Cooper AI. Advances in conjugated microporous polymers. Chem Rev. **120**(4), 2171-2214 (2020). doi:10.1021/acs.chemrev.9b00399